DMD Fast Forward. Published on May 30, 2013 as doi:10.1124/dmd.112.049940

Impact of CYP3A5 Expression on the Inhibition of CYP3A-Catalyzed Drug Metabolism: Considerations for Modeling CYP3A-Mediated Drug-Drug Interactions

Yoshiyuki Shirasaka, Shu-Ying Chang, Mary F. Grubb, Chi-Chi Peng, Kenneth E. Thummel, Nina Isoherranen, and A. David Rodrigues

Department of Pharmaceutics, School of Pharmacy, University of Washington, Seattle, Washington, (Y.S., C.C.P., K.E.T., N.I.) and Pharmaceutical Candidate Optimization, Bristol-Myers Squibb, Princeton, New Jersey (S.Y.C., M.F.G., A.D.R.)

Running title: Impact of CYP3A5 expression on CYP3A-mediated DDIs

Correspondence Address

David Rodrigues, PhD

Metabolism & Pharmacokinetics

Bristol-Myers Squibb, Mail stop F12-04

P.O. Box 4000

Princeton, New Jersey, 08543

USA

david.rodrigues@bms.com

TEL: (609) 252-7813

FAX: (609) 252-6802

Number of text pages:	43
Number of tables:	4
Number of figures:	2
Number of references:	39
Number of words in *Abstract*:	248
Number of words in *Introduction*:	750
Number of words in *Discussion*:	1,341

[1]*Abbreviations*: P450, cytochrome P450; CYP3A4, cytochrome P450 3A4; CYP3A5, cytochrome P450 3A5; rCYP3A4, recombinant cytochrome P450 3A4; rCYP3A5, recombinant cytochrome P450 3A5; MDZ, midazolam; TST, testosterone, ITZ,

itraconazole; KTZ, ketoconazole; HLM, human liver microsomes; 1'OH-MDZ, 1'-hydroxy midazolam; 6βOH-TST, 6β-hydroxy testosterone; K_s, spectral binding constant; K_i, inhibition constant; [I], inhibitor concentration; DDI, drug-drug interaction; IC_{50}, concentration rendering half-maximal inhibition; [*S*], substrate concentration.

DMD Fast Forward. Published on May 30, 2013 as DOI: 10.1124/dmd.112.049940
This article has not been copyedited and formatted. The final version may differ from this version.

Abstract

The purpose of this study was to determine the impact of CYP3A5 expression on inhibitory potency (K_i or IC_{50} values) of CYP3A inhibitors, using recombinant CYP3A4 and CYP3A5 (rCYP3A4 and rCYP3A5) and *CYP3A5* genotyped human liver microsomes (HLMs). IC_{50} ratios between rCYP3A4- and rCYP3A5 (rCYP3A5/rCYP3A4) of ketoconazole (KTZ) and itraconazole (ITZ) were 8.5 and 8.8 for midazolam, 4.7 and 9.1 for testosterone, 1.3 and 2.8 for terfenadine, and 0.6 and 1.7 for vincristine, respectively, suggesting substrate and inhibitor-dependent selectivity of the two azoles. Due to the difference in the IC_{50} values for CYP3A4 and CYP3A5, non-concordant expression of CYP3A4 and CYP3A5 protein can significantly affect the observed magnitude of CYP3A-mediated drug-drug interactions in humans. Indeed, the IC_{50} values of KTZ and ITZ for CYP3A-catalyzed MDZ and TST metabolism were significantly higher in HLMs with *CYP3A5*1/*1* and *CYP3A5*1/*3* genotypes than in HLMs with *CYP3A5*3/*3* genotype, showing CYP3A5 expression-dependent IC_{50} values. Moreover, when IC_{50} values of KTZ and ITZ for different HLMs were kinetically simulated based on CYP3A5 expression level and enzyme-specific IC_{50} values, a good correlation between the simulated and the experimentally measured IC_{50} values was observed. Further simulation analysis revealed that both the K_i ratio (for inhibitors) and V_{max}/K_m ratio (for substrates) between CYP3A4 and CYP3A5 were major factors for CYP3A5 expression-dependent IC_{50} values. In conclusion, the present study demonstrates that CYP3A5 genotype and expression level have a significant impact on inhibitory potency for CYP3A-catalyzed drug metabolism, but that the magnitude of its effect is inhibitor-substrate pair specific.

DMD Fast Forward. Published on May 30, 2013 as DOI: 10.1124/dmd.112.049940
This article has not been copyedited and formatted. The final version may differ from this version.

Introduction

Cytochrome P450 3A (CYP3A) is an important P450 subfamily, because its members are expressed in many tissues and metabolize more than 50% of marketed drugs. Importantly, CYP3A4 is highly expressed in human intestine and liver and is often the locus of drug-drug interactions (DDI) (Thummel and Wilkinson 1998; Lown et al., 1994). A structurally related isoform CYP3A5 is polymorphically expressed in the human intestine and liver in different populations and exhibits an overlapping substrate specificity with that of CYP3A4 (Huang et al., 2004; Lamba et al., 2002). Consequently, it has become increasingly necessary to consider the impact of "CYP3A5 expresser" status on the pharmacokinetic and DDI profiles of CYP3A substrates (Isoherranen et al., 2008; Chandel et al., 2009).

With greater access to recombinant CYP3A (rCYP3A) proteins and human liver microsome (HLM) preparations of *CYP3A5* genotyped subjects, attempts have been made to compare the catalytic and inhibitory properties of CYP3A4 with those of CYP3A5 (Huang et al., 2004; Yamaori et al., 2004; Williams et al., 2002). It is accepted that the majority of CYP3A substrates favor CYP3A4, when the two P450s are incubated under similar assay conditions and one carefully considers their catalytic efficiency in light of redox partner molar ratios (Christensen et al., 2011; Jushchyshyn et al., 2005; Lee and Goldstein, 2012). To date, only drugs such as vincristine (rCYP3A5/rCYP3A4 V_{max}/K_m ratio $\geq$ 8) and tacrolimus (rCYP3A5/rCYP3A4 V_{max}/K_m ratio ~2) favor rCYP3A5 (Niwa et al., 2008; Dennison et al., 2006; Dai et al., 2006). In agreement, CYP3A5 expresser status is a major determinant of vincristine M1 formation *in vitro* and *in vivo* (Dennison et al., 2007, 2008, Egbelakin et al., 2001). Likewise, the respective *in*

vivo (oral) clearance and the HLM-scaled clearance of tacrolimus is 48% and ~60% lower in CYP3A5 nonexpressers, compared to expressors (Dai et al., 2006; Barry and Levine, 2010).

From the standpoint of CYP3A inhibition, azole antifungal agents have been well studied (Gibbs et al., 1999; Isoherranen et al., 2008; Niwa et al., 2008). With some substrates, the IC_{50} ratio (rCYP3A5/rCYP3A4) has been reported to be as high as 19 and implicates CYP3A5 expresser status as an important determinant of K_i in human livers (Niwa et al., 2008, Patki et al., 2003; Isoherranen et al., 2008). Such an observation is supported by the ~2-fold increase in fluconazole K_i with CYP3A5 expresser (versus CYP3A5 non-expresser) HLM (Isoherranen et al., 2008). For itraconazole (ITZ), there are reports that it is rCYP3A4 selective with substrates such as oxybutynin and midazolam (MDZ) (Lukkari et al., 1998; Yamazaki et al., 2010). The latter authors reported a K_i ratio of ~30 (rCYP3A5/rCYP3A4) as well as a K_i ratio of ~2 in HLM (CYP3A5 expressers versus nonexpressers).

Inheritance of at least one copy of the reference CYP3A5 allele (*CYP3A5*1*) confers a significant level of tissue CYP3A5 content, whereas inheritance of two variant alleles (e.g., *CYP3A5*3, CYP3A5*6 or CYP3A5*7*) leads to undetectable or very low CYP3A5 expression (Kuehl et al., 2001). Therefore, the data described above suggest that CYP3A5 expresser status, while not necessarily impacting the overall pharmacokinetics of a particular CYP3A substrate, may govern the [I]/K_i value and the magnitude of a DDI. Clinically, there are at least four reports linking *CYP3A5* genotype to the magnitude of CYP3A inhibition; the impact of KTZ on tacrolimus exposure (Chandel et al., 2009), effect of ITZ on the pharmacokinetics of intravenous MDZ (Yu et al., 2004),

impact of ITZ on the pharmacological activity of clopidogrel (Suh et al., 2006); and the inhibition of MDZ clearance by fluconazole (Isoherranen et al., 2008). Interestingly, Isoherranen et al. (2008) also evaluated the inhibitory effect of fluconazole on erythromycin *N*-demethylase activity in HLM and found that its K_i was not affected by CYP3A5 expression. Clinical follow up revealed no significant association between *CYP3A5* genotype and the magnitude of effect of fluconazole on the erythromycin breath test. This raises the possibility that the impact of CYP3A5 expresser status on the magnitude of a CYP3A-mediated DDI may be substrate-dependent (Isoherranen et al., 2008).

In the present study, we aimed to determine the effect of CYP3A5 expression on the potency of inhibition of CYP3A-catalyzed drug metabolism, by means of *in vitro* studies using rCYP3A4 and rCYP3A5 and nine *CYP3A5* genotyped HLMs together with four representative CYP3A substrates (MDZ, testosterone (TST), terfenadine and vincristine) and two inhibitors (ITZ and KTZ). It is concluded that IC_{50} values for inhibition of CYP3A in HLM are indeed greatly dependent on the expression levels of CYP3A5, and that the quantitative impact of CYP3A5 expression is inhibitor-substrate pair specific.

Materials and Methods

Chemicals and Reagents. Microsomes containing human rCYP3A4 and rCYP3A5 (Supersomes™) were obtained from BD Biosciences (San Jose, California). rCYP3A4 (1.0 nmol CYP3A4/mg) had been co-expressed with cytochrome b_5 (2.8 nmol/mg) and P450 reductase (2.0 µmol cytochrome c reduced/min per mg). rCYP3A5 (1.0 nmol CYP3A5/mg) had been co-expressed with cytochrome b_5 (2.1 nmol/mg) and P450 reductase (3.2 µmol cytochrome c reduced/min per mg). Terfenadine, vincristine, ITZ and KTZ were purchased from Sigma-Aldrich (St. Louis, MO). MDZ and TST were purchased from Cerilliant (Round Rock, TX). All other general reagents were of analytical grade or better and were obtained from various commercial sources. Wild-type purified human CYP3A4, mutant purified human CYP3A4 (L211F/D214E and F213W), P450 reductase and cytochrome b_5 were provided by Drs. James Halpert and Dmitri Davydov (Skaggs School of Pharmacy and Pharmaceutical Sciences, University of California, San Diego, California).

Incubation of rCYP3A4- and rCYP3A5-Catalyzed Metabolism of TST, MDZ, Terfenadine and Vincristine. *Assessment of CYP3A4 and CYP3A5 activity.* All incubations were conducted at 37°C as follows. For the determination of enzyme kinetic parameters, MDZ (0.5-25 µM) was incubated in a reaction mixture (final volume of 0.2 mL) that consisted of the following: rCYP3A4 or rCYP3A5 Supersomes (1 pmol P450/mL), potassium phosphate buffer (100 mM, pH 7.4), EDTA (1 mM) and NADPH (1 mM) for 5 min. The apparent product formation rate with respect to incubation time and protein concentration had previously been determined to be linear. Reactions were

DMD Fast Forward. Published on May 30, 2013 as DOI: 10.1124/dmd.112.049940
This article has not been copyedited and formatted. The final version may differ from this version.

terminated by quenching with one volume of cold acetonitrile containing internal standard, 1'OH-MDZ-d_4. After centrifugation at 4000 x g for 10 min, aliquots of the supernatants were subject to LC/MS/MS analysis. Analysis of 1'OH-MDZ in the incubate extracts was performed using an Accela UHPLC chromatographic system interfaced with an Orbitrap Discovery Mass Spectrometer (Thermofisher, Waltham, MA). Samples (10 µL) were injected via a CTC PAL autosampler (Leap Technologies, Carrboro, NC) into a BEH C18 1.7 µm 2.1 x 100 mm column (Waters Corporation, Milford, MA. The mobile phases were composed of 0.1% formic acid in water (A) and 0.1% formic acid in acetonitrile (B) at a flow rate of 0.6 ml/min. A gradient linearly increased the composition of (B) from 10 to 40% over 6 min, followed by an increase to 95% over the next 2.5 min, maintained at 95% for 1 min, and then returned to initial conditions. Detection of 1'OH-MDZ was achieved in the positive ion electrospray (ESI) mode, with a source voltage of 5.0 kV, a capillary voltage of 15.5 V, and a capillary temperature of 235°C. Tube voltage was set at 50V. Data acquisition was achieved by collecting full scan accurate mass (resolution of 30,000) mass spectra between 100 and 1000 amu. Ion chromatograms of the exact masses of the MH^+ ions of 1'-OH MDZ (342.08103) and 1'-OH MDZ-d_4 (346.10572) were extracted with a mass window of 10 ppm. Peaks in the ion chromatograms were integrated using XCalibur Quan Browser software. The retention times of 1'-OH MDZ and 1'-OH MDZ-d_4 were 4.8 min, while 4-hydroxy MDZ eluted at 4.5 min.

For TST (5-500 µM), enzyme kinetic parameters were determined after incubation with rCYP3A4 or rCYP3A5 Supersomes (10 pmol P450/mL), in potassium phosphate buffer (100 mM, pH 7.4), containing EDTA (1 mM) and NADPH (1 mM) (final volume

of 0.2 mL). Incubation time was 10 min. Again, the apparent product formation rate with respect to incubation time and protein concentration had previously been determined to be linear. Reactions were terminated by transfer of the incubation contents into a Solvinert hydrophobic PTFE filter plate (Millipore, Billerico, MA) preloaded with three volumes of cold methanol containing internal standard, 6βOH-TST-d_3. The filter plate was stacked with a 2 mL injection plate, centrifuged, and the filtrates were subjected to LC/MS/MS analysis. Analysis of 6βOH-TST in incubate extracts was performed using an SCL-10A vp pump (Shimadzu, Columbia, MD) connected to a API4000 Qtrap (AB Sciex, Ontario, Canada). Samples (10 µL) were injected via a CTC PAL autosampler (Leap Technologies, Carrboro, NC) onto a Zorbax (Agilent, Palo Alto, CA) SB-C18 5 µm, 2.1 x 150 mm column. The mobile phases were composed of 0.1% formic acid in water (A) and 0.1% formic acid in methanol (B) at a flow rate of 0.6 ml/min. A gradient linearly increased the composition of (B) from 35% to 80% over 3.5 min., followed by an increase to 100% over the next 0.5 min., maintained at 100% for 1 min. and then returned to initial conditions. Detection of 6βOH-TST was achieved in the positive ion electrospray (ESI) multiple reaction monitoring (MRM) mode, by monitoring *m/z* transitions of 305.2 → 269.2 (6βOH-TST; retention time = 3.04 min) and 308.2 → 272.2 (6βOH-TST-d_3; retention time = 3.03 min). The declustering potential (DP) was set at 66 volts, the collision energy (CE) was set at 21 volts and the turbo-V source temperature was set at 400 °C. Analyst software version 1.4.2 was used for data analysis.

For the determination of enzyme kinetic parameters, terfenadine was incubated for 1 min in a mixture (final volume of 0.2 mL) consisting of the following: rCYP3A4 or rCYP3A5 Supersomes (5 pmol P450/mL), potassium phosphate buffer (100 mM, pH

DMD Fast Forward. Published on May 30, 2013 as DOI: 10.1124/dmd.112.049940
This article has not been copyedited and formatted. The final version may differ from this version.

7.4), EDTA (1 mM) and NADPH (1 mM). The product formation rate with respect to the incubation time and protein concentration had previously been determined to be linear. Reactions were terminated by quenching with one volume of cold acetonitrile containing internal standard, 1'OH-MDZ-d_4. After centrifugation at 4000 x g for 10 min, aliquots of the supernatants were subject to LC/MS/MS analysis. Analysis of terfenadine alcohol in the incubate extracts was performed using an Accela UHPLC chromatographic system interfaced with an Orbitrap Discovery Mass Spectrometer (Thermofisher, Waltham, MA). Samples (10 µL) were injected via a CTC PAL autosampler (Leap Technologies, Carrboro, NC) onto a BEH C18 1.7 µm 2.1 x 100 mm column (Waters Corporation, Milford, MA. The mobile phases were composed of 0.1% formic acid in water (A) and 0.1% formic acid in acetonitrile (B) at a flow rate of 0.6 ml/min A gradient linearly increased the composition of (B) from 2 to 60% over 8 min, up to 95% over the next 0.5 min, maintained at 95% for 0.5 min, and then returned to initial conditions. Detection of terfenadine alcohol was achieved in the positive ion electrospray (ESI) mode, with a source voltage of 5.0 kV, a capillary voltage of 15.5 V, and a capillary temperature of 235. Tube lens voltage was set at 50 V. Data acquisition was achieved by collection of full scan spectrum (mass resolution 30,000), over the range of 100 to 1000 amu. Extracted ion chromatograms of terfenadine alcohol (MH^+ 488.31665) and internal standard 1'-OH MDZ-*d4* (MH^+ 346.10572) were integrated. The retention times of terfenadine alcohol and 1'-OH MDZ-*d4* were 6.3 and 5.3 min, respectively.

For the determination of enzyme kinetic parameters, vincristine was incubated in a reaction mixture that contained rCYP3A4 (50 pmol P450/mL) or rCYP3A5 (10 pmol P450/mL) for 10 min 5 min and 3 min, respectively. The incubation mixture (final

DMD Fast Forward. Published on May 30, 2013 as DOI: 10.1124/dmd.112.049940
This article has not been copyedited and formatted. The final version may differ from this version.

volume of 0.2 mL) also contained potassium phosphate buffer (100 mM, pH 7.4), $MgCl_2$ (1 mM) and NADPH (0.5 mM). The apparent reaction rate was linear with respect to incubation time and protein concentration. Reactions were terminated by the addition of one volume of ice-cold acetonitrile. Concentrations of vincristine metabolite (M1) were determined using UHPLC-MS analysis (Dennison et al., 2006). Analysis of vincristine and M1 in the incubate extracts was performed using an Accela UHPLC pump connected to an LTQ Orbitrap Velos (Thermo Fisher Scientific, Waltham, MA). Samples (10 µL) were injected via a CTC PAL autosampler (Leap Technologies, Carrboro, NC) onto a BEH C18 1.7 µm, 2.1 x 100 mm UPLC column (Waters, Milford, MA). The mobile phases were composed of 0.1% formic acid in water (A) and methanol (B). A gradient linearly increased the composition of (B) from 10% to 40% over six minutes, followed by an increase to 95% over the next 2.5 min. Vincristine eluted at 6.2 min, and metabolite M1 at 5.7 min. The column eluted into the electrospray ion source, heated at 300 °C and operated in the positive mode. Source voltage was set at 5.4 kV. The capillary temperature was set at 300 °C. Sheath and auxiliary gases were operated at 50 and 15 arbitrary units, respectively. Quantitation of vincristine and M1 was accomplished by integration of peak areas in the respective accurate mass ion extracted chromatograms. Masses used were 413.20776 for vincristine and 406.19991 for M1, with windows of 5 ppm. These masses represent the doubly charged states of both molecules and are more abundant than the singly charged species under the conditions described.

Determination of kinetic parameters. All kinetic data were analyzed by nonlinear regression analysis (Kaleida Graph 4.1, Synergy Software, Reading, PA), which involved fitting of the data to equations describing Michaelis-Menten (Eq. 1) or sigmoidal (Eq. 2)

DMD Fast Forward. Published on May 30, 2013 as DOI: 10.1124/dmd.112.049940
This article has not been copyedited and formatted. The final version may differ from this version.

kinetics. In each case, the goodness of the fit was assessed based on visual inspection, assessment of Chi squared, and the standard error of the parameter estimates.

$$v = \frac{V_{max} \times [S]}{K_m + [S]} \quad (1)$$

$$v = \frac{V_{max} \times [S]^n}{S_{50}^n + [S]^n} \quad (2)$$

In equations 1 and 2, "*v*" is the velocity of the metabolic reaction, [*S*] is the substrate concentration and "*n*" is the Hill coefficient.

Inhibition of rCYP3A4 and rCYP3A5 by ITZ and KTZ. KTZ (0.001-5 μM) and ITZ (0.002-10 μM) were studied as inhibitors of rCYP3A4- and rCYP3A5-catalyzed metabolism of MDZ, TST, terfenadine and vincristine. In all cases, the IC_{50} was generated at a [*S*] equivalent to the K_m (S_{50}) and at a [*S*] well below K_m (S_{50}) ([*S*]/K_m ratio ~ 0.05). Both azoles were dissolved in DMSO and the appropriate volume of the stock solution was added to the incubation mixture (final concentration of DMSO did not exceed 0.5%). Incubation and LC/MS/MS analysis was carried out as described for the baseline kinetic studies. Percent of control activity was determined as the ratio of the amount of 1'OH-MDZ, 6βOH-TST, terfenadine alcohol and vincristine M1 formed in the presence to that in the absence (solvent alone) of KTZ or ITZ. IC_{50} values were obtained by means of nonlinear least-squares analysis (Eq. 3) using XLfit (IDBS, Guildford, UK).

$$y = \min + \frac{\max - \min}{1 + \left(\frac{x}{IC_{50}}\right)^{-y}} \quad (3)$$

Where IC_{50} is the "*x*" value for the point in the curve that is midway between the "*max*" (maximum activity remaining; minimal % inhibition) and "*min*" (minimal activity

remaining; maximal % inhibition). The exponent "*y*" is the slope of the curve at its midpoint. *See supplemental data for Determination of Ligand-Induced Binding Spectra and Reconstitution of Purified Wild-Type and Mutant CYP3A4 with P450 Reductase and Cytochrome b_5.*

Inhibition of MDZ 1'-Hydroxylase and TST 6β-Hydroxylase Activity in HLM of CYP3A5 Genotyped Livers. *Microsomal preparations*. The collection and use of human tissue for research was approved by the University of Washington Human Subjects Review Board. Human liver samples were obtained from Human Tissue Bank maintained by School of Pharmacy, University of Washington (Seattle, WA). Of the 60 available livers, 3 from a subset of *CYP3A5*3/*3* donors (1 male; 2 female subjects), 3 from a subset of *CYP3A5*1/*3* donors (3 male donors), were selected randomly from each respective group for microsome preparation. Microsomes from three additional donors genotyped *CYP3A5*1/*1* (1 male; 2 females) were purchased from commercial sources to obtain microsomes from three donors of each genotype (*CYP3A5*1/*1*, *CYP3A5*1/*3* and *CYP3A5*3/*3*). The procedures used for microsome isolation have been published previously (Paine et al., 1997; Lin et al., 2002; Dai et al., 2004). The CYP3A4 and CYP3A5 protein expression levels in each liver were quantified by western blotting and the data is summarized in Table 1. *See supplemental data for Assessment of CYP3A Inhibition and Determination of IC_{50}.*

Simulation of the CYP3A5 Expression-Dependent IC_{50} Values of KTZ and ITZ for MDZ 1'-hydroxylation and TST 6β-Hydroxylation. IC_{50} values of KTZ and ITZ for MDZ 1'-hydroxylation and TST 6β-hydroxylation were simulated to model human liver

DMD Fast Forward. Published on May 30, 2013 as DOI: 10.1124/dmd.112.049940
This article has not been copyedited and formatted. The final version may differ from this version.

microsomes with variable CYP3A4 and CYP3A5 expression. The following model was used (Eq. 4), which assumes that MDZ and TST can be metabolized by CYP3A4 and CYP3A5.

$$\%\ \text{of Control Activity} = \frac{V_i}{V} \times 100 = \frac{\dfrac{V_{\max,CYP3A4} \cdot [E]_{CYP3A4} \cdot [S]}{K_{m,CYP3A4} \cdot \left(1 + \dfrac{[I]}{K_{i,CYP3A4}}\right) + [S]} + \dfrac{V_{\max,CYPA5} \cdot [E]_{CYP3A5} \cdot [S]}{K_{m,CYP3A5} \cdot \left(1 + \dfrac{[I]}{K_{i,CYP3A5}}\right) + [S]}}{\dfrac{V_{\max,CYP3A4} \cdot [E]_{CYP3A4} \cdot [S]}{K_{m,CYP3A4} + [S]} + \dfrac{V_{\max,CYPA5} \cdot [E]_{CYP3A5} \cdot [S]}{K_{m,CYP3A5} + [S]}} \times 100 \quad (4)$$

where [*S*] is the applied concentration of substrate and [*I*] is concentration of inhibitor. $[E]_{CYP3A4}$ and $[E]_{CYP3A5}$ are concentration of CYP3A4 and CYP3A5, respectively in the microsomes. *V* and V_i are metabolite formation velocities in the absence and presence of inhibitor, respectively. By incorporating K_m and V_{max} values of MDZ or TST shown in Table 2, and K_i values estimated from IC_{50} values (K_i = IC_{50} based on a [*S*] that was greater than 10-fold lower than the K_m value) of KTZ or ITZ shown in Table 3, as well as expression levels (concentrations) of CYP3A4 and CYP3A5 to Eq. 4, the percent of control activity ($V_i/V \times 100$) was predicted and the IC_{50} values were determined by nonlinear least-squares analysis using the MULTI program (Yamaoka et al., 1981). Leveraging the IC_{50} values at the low [*S*] circumvents the need to consider different mechanisms of inhibition (competitive versus noncompetitive versus mixed). The relationship between the CYP3A5 expression and the simulated IC_{50} values of KTZ and ITZ for MDZ 1'-hydroxylation and TST 6β-hydroxylation was determined. CYP3A5 expression represents the CYP3A5 specific content (pmol enzyme/mg protein) as a

percentage of a total CYP3A protein content in HLM (CYP3A4 pmol/mg + CYP3A5 pmol/mg).

In addition, the relationship between CYP3A5 expression and IC_{50} values against CYP3A-catalyzed metabolism was simulated using various K_i and V_{max}/K_m ratios (CYP3A5/CYP3A4). The above model (Eq. 4), which assumes that a virtual drug can be metabolized by CYP3A4 and CYP3A5 was used. Simulation of the effect of K_i ratio on CYP3A5 expression-dependent IC_{50} values was performed using kinetic parameters for a virtual CYP3A substrate and inhibitor set as follows: [S] = 100 nM, V_{max}/K_m ratio = 1 and $K_{i,CYP3A4}$ = 100 nM. The effect of V_{max}/K_m ratio on CYP3A5 expression-dependent IC_{50} values was also simulated using kinetic parameters for a virtual CYP3A substrate and inhibitor set as follows: [S] = 100 nM ($<< K_m$) and K_i ratio = 10 ($K_{i,CYP3A4}$ = 100 nM, $K_{i,CYP3A5}$ = 1000 nM).

Statistical Analysis. Data are presented as the mean of values obtained in at least three experiments with the standard deviation (SD). Statistical analyses were performed with the unpaired Student's t-test, and a probability of less than 0.05 ($p < 0.05$) was considered to be statistically significant.

The average fold error (afe) between the simulated and observed IC_{50} values was calculated using equation 5 as described previously for evaluating accuracy of DDI predictions (Brown et al 2005):

$$afe = 10^{\left| \frac{1}{n} \sum \log \frac{Predicte}{Observed} \right|} \quad (5)$$

DMD Fast Forward. Published on May 30, 2013 as DOI: 10.1124/dmd.112.049940
This article has not been copyedited and formatted. The final version may differ from this version.

The difference between the observed and predicted IC_{50} values in the individual livers for each inhibitor-substrate pair were tested using two-tailed paired t-test and a p-value <0.05 was considered significant.

DMD Fast Forward. Published on May 30, 2013 as DOI: 10.1124/dmd.112.049940
This article has not been copyedited and formatted. The final version may differ from this version.

Results

Kinetic Parameters Describing the rCYP3A4- and rCYP3A5-Catalyzed Metabolism of MDZ, TST, Terfenadine, and Vincristine. rCYP3A4 and rCYP3A5 (co-expressed with P450 reductase and cytochrome b_5) were incubated with four different model substrates (TST, MDZ, vincristine and terfenadine) in order to determine the kinetic parameters. In all cases, the rate of metabolite formation was determined under linear conditions and over a suitable substrate concentration range. Under the assay conditions chosen, rCYP3A4- and rCYP3A5-catalyzed formation of 1'OH-MDZ and terfenadine alcohol conformed to Michaelis-Menten (hyperbolic) kinetics (Table 2). On the other hand, vincristine M1 formation with both P450s was best described by sigmoidal kinetics. Only TST 6β-hydroxylation exhibited differential kinetics with rCYP3A4 (sigmoidal) and rCYP3A5 (hyperbolic).

As shown in Table 2, the kinetic parameters for rCYP3A4-catalyzed metabolism of MDZ, TST, terfenadine and vincristine were calculated as 1.8 ± 0.3 μM, 78 ± 34 μM, 3.4 ± 0.4 μM and 75 ± 22 μM (K_m or S_{50} values) and 19 ± 1 pmol/min/pmol, 86 ± 3 pmol/min/pmol, 24 ± 2 pmol/min/pmol and 15 ± 4 pmol/min/pmol (V_{max} values), respectively. The kinetic parameters for rCYP3A5-catalyzed metabolism of MTZ, TST, terfenadine and vincristine were 3.0 ± 0.5 μM, 67 ± 13 μM, 1.5 ± 0.2 μM and 47 ± 7 μM (K_m or S_{50} values) and 35 ± 2 pmol/min/pmol, 56 ± 4 pmol/min/pmol, 18 ± 1 pmol/min/pmol, 70 ± 7 pmol/min/pmol (V_{max} values), respectively. The corresponding V_{max}/K_m (S_{50}) ratios (rCYP3A5/rCYP3A4) for TST, MDZ, terfenadine and vincristine were 0.7, 1.1, 1.7 and 7.5, respectively. This permitted an assessment of CYP3A

DMD Fast Forward. Published on May 30, 2013 as DOI: 10.1124/dmd.112.049940
This article has not been copyedited and formatted. The final version may differ from this version.

inhibition by ITZ and KTZ with a set of model substrates that spanned a 10-fold range of V_{max}/K_m (S_{50}) ratios (rCYP3A5/rCYP3A4).

Inhibition of rCYP3A4 and rCYPA5 by ITZ and KTZ. The inhibitory effect of KTZ and ITZ on rCYP3A4- and rCYP3A5-catalyzed MDZ 1'-hydroxylation, TST 6β-hydroxylation, terfenadine alcohol formation and vincristine M1 formation was analyzed (Supplemental Figs. S1-S4, Table S1 and S2). In each case, IC_{50} values were obtained at a higher (~ K_m) and lower (< K_m) [S]. As expected, the IC_{50} decrease (≥ 11-fold) at the lower [S] was consistent with competitive inhibition. However, for rCYP3A4 with TST (ITZ and KTZ) and vincristine (KTZ), as well as rCYP3A5 with TST (KTZ and ITZ) and vincristine (KTZ), the IC_{50} change was minimal. Such a profile is more consistent with noncompetitive inhibition (Table 3).

As shown in Table 3, the IC_{50} ratios (rCYP3A5/rCYP3A4) of KTZ and ITZ at the higher [S] were 5.0 and 9.6 (MDZ), 4.4 and 33 (TST), 2.2 and 2.3 (terfenadine), and 0.8 and 1.9 (vincristine), respectively, suggesting substrate- and/or inhibitor-dependency for the difference in the IC_{50} values for rCYP3A4- and rCYP3A5-catalyzed drug metabolism. With the exception of the inhibition of TST 6β-hydroxylation by ITZ, similar differences in IC_{50} ratios were observed at the lower [S].

In the present study, rCYP3A4 exhibited sigmoidal kinetics with TST as a substrate, whereas rCYP3A5 did not (Table 2). Therefore, we hypothesized that the large rCYP3A5/rCYP3A4 IC_{50} ratio (33) of ITZ at the higher concentration of TST (~S_{50}) was largely driven by the sigmoidal kinetics exhibited by rCYP3A4 (Table 3). To test the hypothesis, ITZ was evaluated as an inhibitor of wild-type and mutant (L211F/D214E)

DMD Fast Forward. Published on May 30, 2013 as DOI: 10.1124/dmd.112.049940
This article has not been copyedited and formatted. The final version may differ from this version.

CYP3A4. When reconstituted with P450 reductase and cytochrome b_5, the former exhibits sigmoidal kinetics with TST (Hill coefficient n = 1.3). In contrast, TST 6β-hydroxylation catalyzed by the mutant form of CYP3A4 conforms to hyperbolic kinetics (Hill coefficient n = 1). Consequently, at least two amino acid residues (Leu211 and Asp214) are thought to govern the sigmoidal kinetics of CYP3A4 (Harlow and Halpert, 1998). As shown in supplement Table S3 and Supplemental Fig. S6, there was no major difference in the IC_{50} value of ITZ (wild-type versus mutant CYP3A4) when TST was incubated at two concentrations (25 and 100 μM). The higher concentration of TST approximated the S_{50} (~100 μM) of both CYP3A4 forms (Harlow and Halpert, 1998).

To determine whether ITZ and KTZ bind CYP3A4 and CYP3A5 differentially in the absence of a substrate but bind within the active site of CYP3A4 and CYP3A5, ligand-induced difference spectra (binding spectra) were generated with both P450s (Supplemental Fig. S5). Both ITZ and KTZ generated typical Type II binding spectra with rCYP3A4 and rCYP3A5, characteristic of nitrogen coordination to the heme and causing a heme iron high to low spin shift (Kunze et al., 2006; Locuson et al., 2007). However, the maximum change in the magnitude of the ligand-induced spectral change for ITZ was smaller with rCYP3A5 (0.010 AU) than with rCYP3A4 (0.023 AU). For KTZ, the difference in the maximum spectral change between the two P450s was smaller; the maximum absorbance difference was 0.030AU with rCYP3A4 and 0.023AU with rCYP3A5. With regard to ligand affinity, the K_s of ITZ was 118 nM with CYP3A4. The K_s with rCYP3A5 was 3-fold higher (352 nM). For KTZ the determined K_s value for rCYP3A5 (460 nM) was 5-fold higher than the K_s value with CYP3A4 (86 nM).

DMD Fast Forward. Published on May 30, 2013 as DOI: 10.1124/dmd.112.049940
This article has not been copyedited and formatted. The final version may differ from this version.

Inhibitory Effect of ITZ and KTZ on MDZ and TST Metabolism in HLM of *CYP3A5* Genotyped Livers. The inhibitory effect of KTZ and ITZ on CYP3A-catalyzed MDZ 1'-hydroxylation and TST 6β-hydroxylation was evaluated using *CYP3A5* genotyped HLM (Table 1 and Supplemental Figs. S7 and S8). As summarized in Table 4, the IC_{50} values of KTZ and ITZ for MDZ 1'-hydroxylation and TST 6β-hydroxylation varied up to 30-fold between HLMs. Interestingly, the IC_{50} values of KTZ and ITZ were the lowest in the group of HLMs with *CYP3A5*3/*3* genotype, followed by *CYP3A5*1/*1* genotype, and the highest in *CYP3A5*1/*3* genotype. Overall, the IC_{50} values of ITZ towards MDZ and TST were significantly higher in the CYP3A5 expressing livers than in the *CYP3A5*3/*3* livers (Table 4). The IC_{50} values of KTZ towards MDZ were also significantly higher in the CYP3A5 expressing livers than in the *CYP3A5*3/*3* livers, but no significant differences in the IC_{50} values of KTZ for TST metabolism were observed among *CYP3A5* genotypes. Since the expression level of CYP3A5 protein in HLM with *CYP3A5*1/*1* and *CYP3A5*1/*3* genotypes was significantly higher than that in the HLM of livers genotyped *CYP3A5*3/*3*, the IC_{50} values overall appeared to track with the expression level of CYP3A5 (Tables 1 and 4).

By incorporating the kinetic K_m and V_{max} values (Table 2) and K_i (IC_{50} derived) values of KTZ and ITZ (Table 3) for rCYP3A4- and rCYP3A5-catalyzed TST and MDZ metabolism, as well as expression levels of CYP3A4 and CYP3A5 protein in HLM (Table 1) into Eq. (4), the relationship between CYP3A5 expression and IC_{50} values of KTZ and ITZ for CYP3A-catalyzed MDZ and TST metabolisms in individual HLM was simulated (Fig. 1, solid lines). The simulated IC_{50} values were not significantly different from the observed ($p>0.05$ for all inhibitor-substrate pairs), yet the afe analysis showed

DMD Fast Forward. Published on May 30, 2013 as DOI: 10.1124/dmd.112.049940
This article has not been copyedited and formatted. The final version may differ from this version.

that the IC_{50} values of KTZ and ITZ towards TST hydroxylation (afe 0.77 and 0.999 for KTZ and ITZ, respectively) were more accurately predicted than those against MDZ (afe 0.26 and 0.40 for KTZ and ITZ, respectively). Interestingly, the relatively low prediction accuracy for the KTZ-MDZ IC_{50} was independent of the genotype with the predicted IC_{50} –values consistently lower than those observed. In contrast, the discrepancies between predicted and observed values for ITZ-MDZ interaction were mainly driven by the *CYP3A5*1/*1* livers. Of the two azoles tested, the IC_{50} of ITZ was most sensitive to CYP3A5 expression level in HLM (Fig. 1).

Simulation Analysis of the Effect of CYP3A5 Expression on Inhibition of CYP3A-Catalyzed Drug Metabolism.

To consider the effect of the different K_i values of novel CYP3A inhibitors, and V_{max}/K_m values between CYP3A4 and CYP3A5 of CYP3A substrates, on CYP3A5 expression-dependent IC_{50} values, the relationship between CYP3A5 expression and IC_{50} values against CYP3A-catalyzed metabolism was simulated using various K_i and V_{max}/K_m ratios (CYP3A5/CYP3A4) (Fig. 2). The effect of the K_i ratio on CYP3A5 expression-dependent IC_{50} values was simulated using kinetic parameters for a virtual CYP3A substrate and inhibitor set as follows: substrate concentration = 100 nM, V_{max}/K_m ratio = 1 (i.e. CYP3A4 and CYP3A5 have equal intrinsic clearances for the substrate) and $K_{i,CYP3A4}$ = 100 nM (Fig. 2A). When the K_i ratio (CYP3A5/CYP3A4) was 1.0, no effect of CYP3A5 expression on the IC_{50} value for CYP3A-catalyzed drug metabolism was observed. The simulated IC_{50} value increased with increasing relative CYP3A5

DMD Fast Forward. Published on May 30, 2013 as DOI: 10.1124/dmd.112.049940
This article has not been copyedited and formatted. The final version may differ from this version.

expression with an increase in the K_i ratio and conversely decreased with decreased K_i ratio.

Simulation of the effect of CYP3A V_{max}/K_m ratio on CYP3A5 expression-dependent IC_{50} values was also performed using kinetic parameters for a virtual CYP3A substrate and inhibitor set as follows: substrate concentration = 100 nM ($<< K_m$) and K_i ratio = 10 ($K_{i,CYP3A4}$ = 100 nM, $K_{i,CYP3A5}$ = 1000 nM) (Fig. 2B). When the V_{max}/K_m ratio was higher, the IC_{50} value for CYP3A-catalyzed drug metabolism increased even when CYP3A5 expression was low (<20% of total CYP3A). In contrast, when the V_{max}/K_m ratio was lower, the IC_{50} value was constant or slightly changed at lower CYP3A5 levels, then increased at higher CYP3A5 levels. This simulation suggested that variability of IC_{50} values for CYP3A-catalyzed drug metabolism became more sensitive to CYP3A5 expression when CYP3A5 contribution to substrate clearance was greater.

DMD Fast Forward. Published on May 30, 2013 as DOI: 10.1124/dmd.112.049940
This article has not been copyedited and formatted. The final version may differ from this version.

Discussion

The results of this study show that CYP3A5 genotype and protein expression level have a significant impact on the inhibitory potency of ITZ and KTZ, but that the magnitude of the effect is inhibitor-substrate pair specific. The IC_{50} ratios (rCYP3A5/rCYP3A4) of KTZ and ITZ for the inhibition of rCYP3A4- and rCYP3A5-catalyzed metabolism of MDZ and TST were much higher (> 4) than those for terfenadine and vincristine (< 3). This difference in the IC_{50} values for CYP3A4 and CYP3A5 may result in a complex CYP3A-mediated DDI profile in humans carrying the *CYP3A5*1* allele that confers significant expression of the encoded enzyme (Kuehl et al., 2001). It is noteworthy that the range of IC_{50} ratios cannot be rationalized solely on the basis of higher ITZ (~3-fold) and KTZ (~5-fold) CYP3A4 binding affinity (K_s) in the absence of a substrate. This implies that one has to consider the binding of both substrate and inhibitor within the CYP3A active site and the effect of allosterism in substrate dependent inhibitory potency. In agreement with what would be predicted from rCYP data, the IC_{50} values of KTZ and ITZ for MDZ 1'-hydroxylation and for ITZ for TST 6β-hydroxylation were significantly higher in HLMs with *CYP3A5*1/*1* and *CYP3A5*1/*3* genotypes than in HLMs with *CYP3A5*3/*3* genotype. However, no significant difference in the IC_{50} values of KTZ for TST metabolism was observed among the *CYP3A5* genotype groups (Table 4). Based on the higher CYP3A5 protein expression level in HLMs with *CYP3A5*1/*1* and *CYP3A5*1/*3* genotypes compared to *CYP3A5*3/*3* genotype, the greater IC_{50} values of KTZ and ITZ for CYP3A-catalyzed MDZ and TST metabolism is likely due to the higher expression level of CYP3A5 and lower inhibitory potency of KTZ and ITZ towards CYP3A5 than CYP3A4 (higher IC_{50}

DMD Fast Forward. Published on May 30, 2013 as DOI: 10.1124/dmd.112.049940
This article has not been copyedited and formatted. The final version may differ from this version.

ratios) (Tables 1, 3 and 4). Alternatively, one can anticipate no significant effect of CYP3A5 expression on the IC_{50} values of KTZ and ITZ for CYP3A-catalyzed metabolism of terfenadine and vincristine, based on the low IC_{50} ratios of KTZ and ITZ shown in Table 3. Further investigation would be needed to clarify the impact of CYP3A5 expression on the inhibition of CYP3A-catalyzed metabolism of terfenadine and vincristine. Overall, the relative CYP3A5 expression level rather than genotype (heterozygous or homozygous *CYP3A5*1*) determined the magnitude of IC_{50} value of ITZ and KTZ in HLMs.

Results from our simulation of the IC_{50} values at different CYP3A5 expression levels with KTZ and ITZ using kinetic data from CYP3A4 and CYP3A5 Supersomes and protein expression levels of CYP3A4 and CYP3A5 in the HLMs support our conclusion that relative CYP3A5 expression determines the inhibitory potency towards a given substrate (Fig. 1). When the simulated IC_{50} values of KTZ and ITZ were compared to the experimentally measured IC_{50} values, the predicted IC_{50} values were not significantly different from each other, demonstrating that simulation can be used to predict the effect of CYP3A5 expression on the IC_{50} values for CYP3A-catalyzed drug metabolism (Fig. 1). Interestingly the prediction of the IC_{50}-values was more accurate for both inhibitors when TST was used as a substrate than with MDZ (afe 0.32 versus 0.87). This difference in prediction accuracy could be due to unaccounted allosteric, substrate specific effects. Such allosteric effects were recently shown in vitro and in vivo between fluconazole and MDZ (Yang et al 2012). However, for both MDZ and TST metabolism, the observed IC_{50} values were generally within the two-fold range of the predicted values with the exception of HL150. In this donor the observed IC_{50} –value was significantly higher than

DMD Fast Forward. Published on May 30, 2013 as DOI: 10.1124/dmd.112.049940
This article has not been copyedited and formatted. The final version may differ from this version.

that predicted and that observed in the other donors. One of the possible explanations for this inconsistency is the potential contribution of CYP3A7 to drug metabolism in HLM150 and relatively weak inhibition of CYP3A7 by KTZ and ITZ, yielding a higher IC_{50} value of KTZ and ITZ for MDZ and TST metabolism (Nishimura et al., 2003; Sim et al., 2005; Hata et al., 2010). Such a hypothesis is supported by the much higher (~16-fold) IC_{50} of KTZ for rCYP3A7-catalyzed TST metabolism versus rCYP3A5 (630 nM versus 40 nM; data not shown). Another possible explanation is that, minor contributions from other P450 enzymes to MDZ and TST metabolism, such as CYP2C9 and CYP2C19, may be factors in the deviation (Choi et al., 2005).

In order to further evaluate the potential impact of CYP3A5 expression in CYP3A IC_{50} values, the effect of K_i ratios (CYP3A5/CYP3A4) of CYP3A inhibitors and V_{max}/K_m ratios (CYP3A5/CYP3A4) of CYP3A substrates on CYP3A5 expression-dependent IC_{50} values was simulated. As shown in Fig. 2A, a CYP3A5 expression-dependent change in the IC_{50} values for CYP3A-catalyzed drug metabolism was clearly predicted when the K_i ratio deviates from 1, whereas no effect of CYP3A5 expression on IC_{50} value is expected when the K_i ratio is unity. Therefore, it is concluded that K_i ratio is one of the major determinants for CYP3A5 expression-dependent IC_{50} values. On the other hand, as shown in Fig. 2B, the effect of CYP3A5 expression on the IC_{50} value for CYP3A-catalyzed drug metabolism is also dependent on the relative catalytic efficiency of CYP3A5 when compared to CYP3A4 and more sensitive at higher CYP3A5/CYP3A4 V_{max}/K_m ratios. Accordingly, if the contribution of CYP3A5 to total CYP3A-catalyzed drug metabolism is high (that is, the intrinsic clearance of the drug is higher for CYP3A5 than for CYP3A4), even very low relative CYP3A5 expression has a significant effect on

DMD Fast Forward. Published on May 30, 2013 as DOI: 10.1124/dmd.112.049940
This article has not been copyedited and formatted. The final version may differ from this version.

observed apparent IC_{50} values. In such a case CYP3A5 expression would again become an important factor to consider when determining IC_{50} values for CYP3A-catalyzed drug metabolism in HLMs. However, if the contribution of CYP3A5 to total CYP3A-catalyzed drug metabolism is low i.e. intrinsic clearance of CYP3A5~0.1 (Fig 2), the effect of an individual difference in CYP3A5 expression on the IC_{50} values is likely to be negligible, despite any difference in the K_i value for CYP3A4 and CYP3A5.

The present findings suggest that when CYP3A-mediated DDI studies are planned, the inhibition potency of the new chemical entity towards CYP3A4 and CYP3A5 should be tested *in vitro* using the same probe as will be used in the clinical study to determine whether *CYP3A5* genotype will affect interindividual variability in the magnitude of the DDI observed and significantly affect study power. The inhibitor selectivity should be considered in relation to the intrinsic clearance ratio of the substrate. The influence of CYP3A5 expression on the magnitude of DDIs could also be taken into consideration when the *in vivo* probe substrate is selected. On the other hand, when the new chemical entity is considered as the object drug of the DDI, it will be prudent to determine the contribution of CYP3A5 to the overall clearance of the drug (in CYP3A5 expressors) and to test the effect of CYP3A5 expression on the IC_{50} of KTZ or another strong CYP3A inhibitor towards that specific compound. It is important to note that due to the allosteric behavior of CYP3A, the effect of CYP3A5 expression on *in vivo* IC_{50} values is specific for the inhibitor-substrate pair and needs to be determined individually *in vitro* for the combination in the study. Unfortunately, very few compounds have been studied *in vivo* or *in vitro* for their potency as CYP3A5 inhibitors and, as such, extrapolation of these data to the overall variability of the magnitude of CYP3A-mediated DDIs can be

DMD Fast Forward. Published on May 30, 2013 as DOI: 10.1124/dmd.112.049940
This article has not been copyedited and formatted. The final version may differ from this version.

challenging. This is emphasized with the fact that at present very limited data are available for CYP3A5 contribution to the clearance of the known sensitive substrates of CYP3A. More systematic studies are needed to establish the overall clinical significance of CYP3A5 inhibition in clinical DDIs.

In conclusion, the present study demonstrates that the IC_{50} value for CYP3A-catalyzed drug metabolism measured using HLMs varies due to difference in CYP3A5 expression/genotype, the substrate studied and the relative inhibitory potency towards CYP3A4 and CYP3A5. These findings imply that the HLM assay has potential to misread the IC_{50} value for CYP3A-catalyzed drug metabolism. However, simulation analysis, as described in the present study, may be useful when considering variability of IC_{50} values for CYP3A-catalyzed drug metabolism in individual HLMs and enable relatively precise prediction of DDIs *in vivo* involving the inhibition of CYP3A.

DMD Fast Forward. Published on May 30, 2013 as DOI: 10.1124/dmd.112.049940
This article has not been copyedited and formatted. The final version may differ from this version.

Acknowledgements

The authors would like to thank Drs. James Halpert and Dmitri Davydov (Skaggs School of Pharmacy and Pharmaceutical Sciences, University of California, San Diego, California) for the kind gifts of purified human CYP3A4 (wild-type and mutant forms), P450 reductase and cytochrome b_5.

Authorship contributions:

Participated in study design: Isoherranen, Thummel, Rodrigues

Conducted experiments: Peng, Grubb, Chang, Shirasaka

Performed data analysis: Shirasaka, Chang, Grubb, Isoherranen, Rodrigues

Wrote or contributed to the writing of the manuscript: Shirasaka, Rodrigues, Thummel, Isoherranen, Chang, Grubb

References

Barry A and Levine M (2010) A systematic review of the effect of CYP3A5 genotype on the apparent oral clearance of tacrolimus in renal transplant recipients. *Ther Drug Monit* **32**:708-714.

Brown HS, Ito K, Galetin A, and Houston B (2005) Prediction of *in vivo* drug–drug interactions from *in vitro* data: impact of incorporating parallel pathways of drug elimination and inhibitor absorption rate constant, *Br J Clin Pharmacol*, **60**: 508-518

Chandel N, Aggarwal PK, Minz M, Sakhuja V, Kohli KK, and Jha V (2009) CYP3A5*1/*3 genotype influences the blood concentration of tacrolimus in response to metabolic inhibition by ketoconazole. *Pharmacogenet Genomics* **19**:458-463.

Choi MH, Skipper PL, Wishnok JS, and Tannenbaum SR (2005) Characterization of testosterone 11 beta-hydroxylation catalyzed by human liver microsomal cytochromes P450. *Drug Metab Dispos* **33**:714-718.

Christensen H, Hestad AL, Molden E, and Mathiesen L (2011) CYP3A5-mediated metabolism of midazolam in recombinant systems is highly sensitive to NADPH-cytochrome P450 reductase activity. *Xenobiotica* **41**:1-5.

Dai Y, Iwanaga K, Lin YS, Hebert MF, Davis CL, Huang W, Kharasch ED, and Thummel KE (2004) In vitro metabolism of cyclosporine A by human kidney CYP3A5. *Biochem Pharmacol* **68**:1889-1902.

Dai Y, Hebert MF, Isoherranen N, Davis CL, Marsh C, Shen DD, and Thummel KE (2006) Effect of CYP3A5 polymorphism on tacrolimus metabolic clearance in vitro. *Drug Metab Dispos* **34**:836-47.

Dennison JB, Kulanthaivel P, Barbuch RJ, Renbarger JL, Ehlhardt WJ, and Hall SD (2006) Selective metabolism of vincristine in vitro by CYP3A5. *Drug Metab Dispos* **34**:1317-1327.

Dennison JB, Jones DR, Renbarger JL, and Hall SD (2007) Effect of CYP3A5 expression on vincristine metabolism with human liver microsomes. *J Pharmacol Exp Ther* **32**:553-563.

Dennison JB, Mohutsky MA, Barbuch RJ, Wrighton SA, and Hall SD (2008) Apparent high CYP3A5 expression is required for significant metabolism of vincristine by human cryopreserved hepatocytes. *J Pharmacol Exp Ther* **27**:248-257.

Domanski TL, He YA, Khan KK, Roussel F, Wang Q, and Halpert JR (2001) Phenylalanine and tryptophan scanning mutagenesis of CYP3A4 substrate recognition site residues and effect on substrate oxidation and cooperativity. *Biochemistry* **40**:10150-10160.

Egbelakin A, Ferguson MJ, MacGill EA, Lehmann AS, Topletz AR, Quinney SK, Li L, McCammack KC, Hall SD, and Renbarger JL (2009) Increased risk of vincristine neurotoxicity associated with low CYP3A5 expression genotype in children with acute lymphoblastic leukemia. *Pediatr Blood Cancer* **56**:361-367.

Gibbs MA, Thummel KE, Shen DD, and Kunze KL (1999) Inhibition of cytochrome P-450 3A (CYP3A) in human intestinal and liver microsomes: comparison of K_i values and impact of CYP3A5 expression. *Drug Metab Dispos* **27**:180-187.

Hata S, Miki Y, Fujishima F, Sato R, Okaue A, Abe K, Ishida K, Akahira J, Unno M, and Sasano H (2010) Cytochrome 3A and 2E1 in human liver tissue: Individual variations among normal Japanese subjects. *Life Sci* **86**:393-401.

Harlow GR and Halpert JR (1998) Analysis of human cytochrome P450 3A4 cooperativity: construction and characterization of a site-directed mutant that displays hyperbolic steroid hydroxylation kinetics. *Proc Natl Acad Sci U S A* **95**: 6636-6641.

Huang W, Lin YS, McConn DJ, Calamia JC, Totah RA, Isoherranen N, Glodowski M, and Thummel KE (2004). Evidence of significant contribution from CYP3A5 to hepatic drug metabolism. *Drug Metab Dispos* **32**:1434-1445.

Isoherranen N, Ludington SR, Givens RC, Lamba JK, Pusek SN, Dees EC, Blough DK, Iwanaga K, Hawke RL, Schuetz EG, Watkins PB, Thummel KE, and Paine MF (2008) The influence of CYP3A5 expression on the extent of hepatic CYP3A inhibition is substrate-dependent: an in vitro-in vivo evaluation. *Drug Metab Dispos* **36**:146-154.

Jushchyshyn MI, Hutzler JM, Schrag ML, and Wienkers LC (2005) Catalytic turnover of pyrene by CYP3A4: evidence that cytochrome b_5 directly induces positive cooperativity. *Arch Biochem Biophys* **438**:21-28.

Kuehl P, Zhang J, Lin Y, Lamba J, Assem M, Schuetz J, Watkins PB, Daly A, Wrighton SA, Hall SD, Maurel P, Relling M, Brimer C, Yasuda K, Venkataramanan R, Strom S, Thummel K, Boguski MS, and Schuetz E (2001) Sequence diversity in CYP3A promoters and characterization of the genetic basis of polymorphic CYP3A5 expression. *Nat Genet* **27**:383–391.

Kunze KL, Nelson WL, Kharasch ED, Thummel KE, and Isoherranen N (2006) Stereochemical aspects of itraconazole metabolism in vitro and in vivo. *Drug Metab Dispos* **34**:583-590.

Lamba JK, Lin YS, Schuetz EG, and Thummel KE (2002) Genetic contribution to variable human CYP3A-mediated metabolism. *Adv Drug Deliv Rev* **54**:1271-1294.

Lee S-J and Goldstein JA (2012) Comparison of CYP3A4 and CYP3A5: the effects of cytochrome b_5 and NADPH-cytochrome P450 reductase on testosterone hydroxylation activities. *Drug Metab and Pharmacokinet* [Advance Publication] Released: June 12, 2012.

Locuson CW, Hutzler JM, and Tracy TS (2007) Visible spectra of type II cytochrome P450-drug complexes: evidence that "incomplete" heme coordination is common. *Drug Metab Dispos* **35**:614-622.

Lin YS, Dowling AL, Quigley SD, Farin FM, Zhang J, Lamba J, Schuetz EG, and Thummel KE (2002) Co-regulation of CYP3A4 and CYP3A5 and contribution to hepatic and intestinal midazolam metabolism. *Mol Pharmacol* **62**:162-172.

Lown KS, Kolars JC, Thummel KE, Barnett JL, Kunze KL, Wrighton SA, and Watkins PB (1994) Interpatient heterogeneity in expression of CYP3A4 and CYP3A5 in small bowel. Lack of prediction by the erythromycin breath test. *Drug Metab Dispos* **22**:947-955.

Lukkari E, Taavitsainen P, Juhakoski A, and Pelkonen O (1998) Cytochrome P450 specificity of metabolism and interactions of oxybutynin in human liver microsomes. *Pharmacol Toxicol* **82**:161-166.

Nishimura M, Yaguti H, Yoshitsugu H, Naito S, and Satoh T (2003) Tissue distribution of mRNA expression of human cytochrome P450 isoforms assessed by high-sensitivity real-time reverse transcription PCR. *Yakugaku Zasshi* **123**:369-375.

Niwa T, Murayama N, Emoto C, and Yamazaki H (2008) Comparison of kinetic parameters for drug oxidation rates and substrate inhibition potential mediated by cytochrome P450 3A4 and 3A5. *Curr Drug Metab* **9**:20-33.

Paine MF, Khalighi M, Fisher JM, Shen DD, Kunze KL, Marsh CL, Perkins JD, and Thummel KE (1997) Characterization of interintestinal and intraintestinal variations in human CYP3A-dependent metabolism. *J Pharmacol Exp Ther* **283**:1552-1562.

Patki KC, Von Moltke LL, and Greenblatt DJ (2003) In vitro metabolism of midazolam, triazolam, nifedipine, and testosterone by human liver microsomes and recombinant cytochromes P450: role of CYP3A4 and CYP3A5. *Drug Metab Dispos* **31**:938-944.

Sim SC, Edwards RJ, Boobis AR, and Ingelman-Sundberg M (2005) CYP3A7 protein expression is high in a fraction of adult human livers and partially associated with the CYP3A7*1C allele. *Pharmacogenet Genomics.* **15**:625-631.

Suh JW, Koo BK, Zhang SY, Park KW, Cho JY, Jang IJ, Lee DS, Sohn DW, Lee MM, and Kim HS (2006) Increased risk of atherothrombotic events associated with cytochrome P450 3A5 polymorphism in patients taking clopidogrel. *CMAJ* **174:**1715-1722.

Thummel KE and Wilkinson GR (1998) In vitro and in vivo drug interactions involving CYP3A. *Annu Rev Pharmacol Toxicol* **38**: 389-430.

Williams JA, Ring BJ, Cantrell VE, Jones DR, Eckstein J, Ruterbories K, Hamman MA, Hall SD, and Wrighton SA (2002) Comparative metabolic capabilities of CYP3A4, CYP3A5, and CYP3A7. *Drug Metab Dispos* **30**:883-891.

Yang J, Atkins WM, Isoherranen N, Paine MF, Thummel KE. (2012) Evidence of CYP3A allosterism in vivo: analysis of interaction between fluconazole and midazolam *Clin Pharmacol Ther.* **91**:442-449

Yamaoka K, Tanigawara Y, Nakagawa T, and Uno T (1981) A pharmacokinetic analysis program (multi) for microcomputer. *J Pharmacobiodyn* **4**: 879-885.

Yamaori S, Yamazaki H, Iwano S, Kiyotani K, Matsumura K, Honda G, Nakagawa K, Ishizaki T, and Kamataki T (2004) CYP3A5 Contributes significantly to CYP3A-mediated drug oxidations in liver microsomes from Japanese subjects. *Drug Metab Pharmacokinet* **19**:120-129.

Yamazaki H, Nakamoto M, Shimizu M, Murayama N, and Niwa T (2010) Potential impact of cytochrome P450 3A5 in human liver on drug interactions with triazoles. *Br J Clin Pharmacol* **69**:593-597.

Yu KS, Cho JY, Jang IJ, Hong KS, Chung JY, Kim JR, Lim HS, Oh DS, Yi SY, Liu KH, Shin JG, and Shin SG (2004) Effect of the CYP3A5 genotype on the pharmacokinetics of intravenous midazolam during inhibited and induced metabolic states. *Clin Pharmacol Ther* **76**:104-112.

Footnote

This work was supported in part by a Postdoctoral Fellowship for Research Abroad from Japan Society for the Promotion of Science [Research Project Number: H23-694] and National Institutes of Health grant [P01 GM32165].

DMD Fast Forward. Published on May 30, 2013 as DOI: 10.1124/dmd.112.049940
This article has not been copyedited and formatted. The final version may differ from this version.

Figure Legends

Figure 1. Relationship between CYP3A5 expression and IC_{50} values of KTZ and ITZ for the CYP3A-catalyzed metabolism of MDZ and TST in HLM.

Relationship between CYP3A5 expression and IC_{50} value of KTZ (A) and ITZ (B) for MDZ and KTZ (C) and ITZ (D) for TST metabolism... CYP3A5 expression represents CYP3A5 protein expression (pmol/mg) as a percentage of a total CYP3A protein expression in HLM (CYP3A4 pmol/mg + CYP3A5 pmol/mg). Solid and dotted lines represent simulated data and its two-fold error ranges, respectively (see *Materials and Methods*); solid circles, triangles and squares represent observed data using HLMs with *CYP3A5*1/*1*, *CYP3A5*1/*3* and *CYP3A5*3/*3* genotypes, respectively. Data are presented as mean ± SD (n = 3 determinations).

Figure 2. Simulation analysis of effect of CYP3A5 expression on inhibition of CYP3A-catalyzed drug metabolism.

(A) Impact of K_i ratio (CYP3A5/CYP3A4) on CYP3A5 expression-dependent IC_{50} values. Kinetic parameters for a virtual CYP3A substrate and inhibitor used in current simulations are set as follows: substrate concentration = 100 nM, V_{max}/K_m ratio = 1 and $K_{i,CYP3A4}$ = 100 nM. (B) Impact of V_{max}/K_m ratio (CYP3A5/CYP3A4) on CYP3A5 expression-dependent IC_{50} values. Kinetic parameters for a virtual CYP3A substrate and inhibitor used in current simulations are set as follows: substrate concentration = 100 nM ($<< K_m$) and K_i ratio = 10 ($K_{i,CYP3A4}$ = 100 nM, $K_{i,CYP3A5}$ = 1000 nM). CYP3A5 expression represents the percentage of total CYP3A (CYP3A4 + CYP3A5) expression (see Materials and Methods).

Table 1.

Differential Expression of CYP3A4 and CYP3A5 Protein in Various HLM Preparations

CYP3A5 Genotype	HLM Preparation	Expression Level		
		CYP3A4 (pmol/mg)	CYP3A5 (pmol/mg)	Percentage of CYP3A5 [a] (%)
**1/*1*	HH739	11.0	6.00	35.3
	HH867	110	17.0	13.4
	HH47	62.0	9.30	13.0
	Mean ± S.D.	61.0 ± 49.5	10.8 ± 5.6*	20.6 ± 12.7
**1/*3*	HL150	5.00	22.0	81.5
	HL125	72.0	58.0	44.6
	HL167	19.0	33.0	63.5
	Mean ± S.D.	32.0 ± 35.3	37.7 ± 18.4*	63.2 ± 18.4*
**3/*3*	HL152	25.0	1.00	3.80
	HL143	38.0	1.00	2.60
	HL131	28.0	1.00	3.40
	Mean ± S.D.	30.3 ± 6.8	1.00 ± 0.00	3.29 ± 0.66

HL: human liver.

[a] CYP3A5 expression represents CYP3A5 protein expression (pmol/mg) as a percentage of a total CYP3A protein expression in HLM (CYP3A4 pmol/mg + CYP3A5 pmol/mg). **P* < 0.05, significantly different from expression level of CYP3A5 in HLM of a liver genotyped *CYP3A5*3/*3*. Data are represented as mean ± S.D. (n = 3 determinations).

Table 2.

Kinetic Parameters for the rCYP3A4- and rCYP3A5-Catalyzed Metabolism of MDZ, TST, Terfenadine and Vincristine

CYP	Substrate	Model	K_m (S_{50}) (μM)	V_{max}[a]	n[c]	$V_{max}/K_m(S_{50})$	V_{max}/K_m (S_{50}) Ratio[b]
CYP3A4	MDZ	Hyperbolic	1.8 ± 0.3	19 ± 1	-	11.0	
	TST	Sigmoidal	78 ± 34	86 ± 3	1.2 ± 0.13	1.1	
	Terfenadine	Hyperbolic	3.4 ± 0.4	24 ± 2	-	7	
	Vincristine	Sigmoidal	75 ± 22	15 ± 4	1.5 ± 0.15	0.2	
CYP3A5	MDZ	Hyperbolic	3.0 ± 0.5	35 ± 2	-	11.7	1.1
	TST	Hyperbolic	67 ± 13	56 ± 4	-	0.8	0.7
	Terfenadine	Hyperbolic	1.5 ± 0.2	18 ± 1	-	12.0	1.7
	Vincristine	Sigmoidal	47 ± 6.7	70 ± 7	1.5 ± 0.11	1.5	7.5

[a]Presented as pmol/min per pmol P450, except for the formation of vincristine M1 metabolite. No attempt was made to formally quantitate M1, so data are presented as arbitrary units (see *Materials and Methods*). [b]Ratio of CYP3A5 V_{max}/K_m (S_{50}) versus CYP3A4 V_{max}/K_m (S_{50}). [c]Hill coefficient. Data are represented as mean ± S.D. (n = 3 determinations), except for the CYP3A5/CYP3A4 V_{max}/K_m (S_{50}) ratio.

Table 3.

KTZ and ITZ as Inhibitors of MDZ, TST, Terfenadine, and Vincristine Metabolism

MDZ, TST, Terfenadine, and Vincristine

Substrate	P450	Substrate Conc. (μM)[d]	IC_{50} (nM)[a]		CYP3A5/CYP3A4 IC_{50} Ratio	
			KTZ	ITZ	KTZ	ITZ
MDZ	rCYP3A4	1.4 (0.8)	40 ± 10	240 ± 50	5.0[b]	9.6
		0.1 (0.06)	2.0 ± 0.2	17 ± 3	8.5[c]	8.8
	rCYP3A5	2.7 (0.9)	200 ± 4	2300 ± 400		
		0.2 (0.07)	17 ± 3	150 ± 60		
TST	rCYP3A4	78 (1.0)	9.0 ± 1	40 ± 7	4.4	33
		4.0 (0.05)	17 ± 1	45 ± 3	4.7	9.1
	rCYP3A5	67 (1.0)	40 ± 6	1300 ± 400		
		3.0 (0.04)	80 ± 7	410 ± 180		
Terfenadine	rCYP3A4	2.4 (0.7)	90 ± 5	900 ± 200	2.2	2.3
		0.2 (0.06)	8.2 ± 1	23 ± 4	1.3	2.8
	rCYP3A5	1.2 (0.8)	200 ± 5	2100 ± 500		
		0.1 (0.07)	6.5 ± 2	64 ± 14		
Vincristine	rCYP3A4	75 (1.0)	150 ± 30	360 ± 50	0.8	1.9
		4.0 (0.05)	111 ± 10	29 ± 4	0.6	1.7
	rCYP3A5	45 (1.0)	120 ± 10	680 ± 230		
		2.0 (0.04)	70 ± 10	50 ± 5		

[a] IC_{50} was determined at a [S] close to the K_m (S_{50}) and at a [S] below K_m (S_{50}) (see Table 2). The data are represented as mean ± S.D. (n = 3 determinations).

[b]IC_{50} ratio at higher [S]. [c]IC_{50} ratio at lower [S]. [d][S]/K_m ratio in parentheses.

Table 4.

Impact of CYP3A5 Expression on the Inhibition of MDZ and TST Metabolism in HLM by KTZ and ITZ

CYP3A5 Genotype	HLM Preparation	IC_{50} (nM) MDZ [a] + KTZ	MDZ [a] + ITZ	TST [b] + KTZ	TST [b] + ITZ
	HL739	35.8 ± 3.8	108 ± 24	31.5 ± 4.8	85.4 ± 10.5
*1/*1	HL867	34.3 ± 3.2	111 ± 15	19.7 ± 3.8	120 ± 12
	HL47	30.7 ± 4.0	123 ± 21	29.1 ± 2.7	111 ± 11
Mean ± S.D.		33.6 ± 2.6*	114 ± 8*	26.8 ± 6.3	105 ± 18*
	HL150	132 ± 13	1133 ± 782	308 ± 52	513 ± 105
*1/*3	HL125	11.8 ± 1.5	161 ± 27	53.9 ± 3.8	158 ± 14
	HL167	24.3 ± 2.2	176 ± 13	64.2 ± 6.6	195 ± 15
Mean ± S.D.		56.1 ± 66.3	490 ± 557	142 ± 144	289 ± 195*
	HL152	6.92 ± 1.12	47.3 ± 8.5	25.8 ± 3.8	20.0 ± 2.3
*3/*3	HL143	12.9 ± 2.0	83.0 ± 5.9	27.1 ± 5.5	21.6 ± 1.7
	HL131	11.5 ± 1.0	53.3 ± 7.4	10.2 ± 1.1	46.7 ± 4.2
Mean ± S.D.		10.4 ± 3.1	61.2 ± 19.1	21.0 ± 9.4	29.4 ± 15.0

[a] Initial concentration of MDZ was 1 μM. [b] Initial concentration of TST was 10 μM. *$P < 0.05$, significantly different from the IC_{50} obtained with HLM of a liver genotyped *CYP3A5*3/*3*. Data are represented as mean ± S.D. (n = 3 determinations).

HL: Human liver.

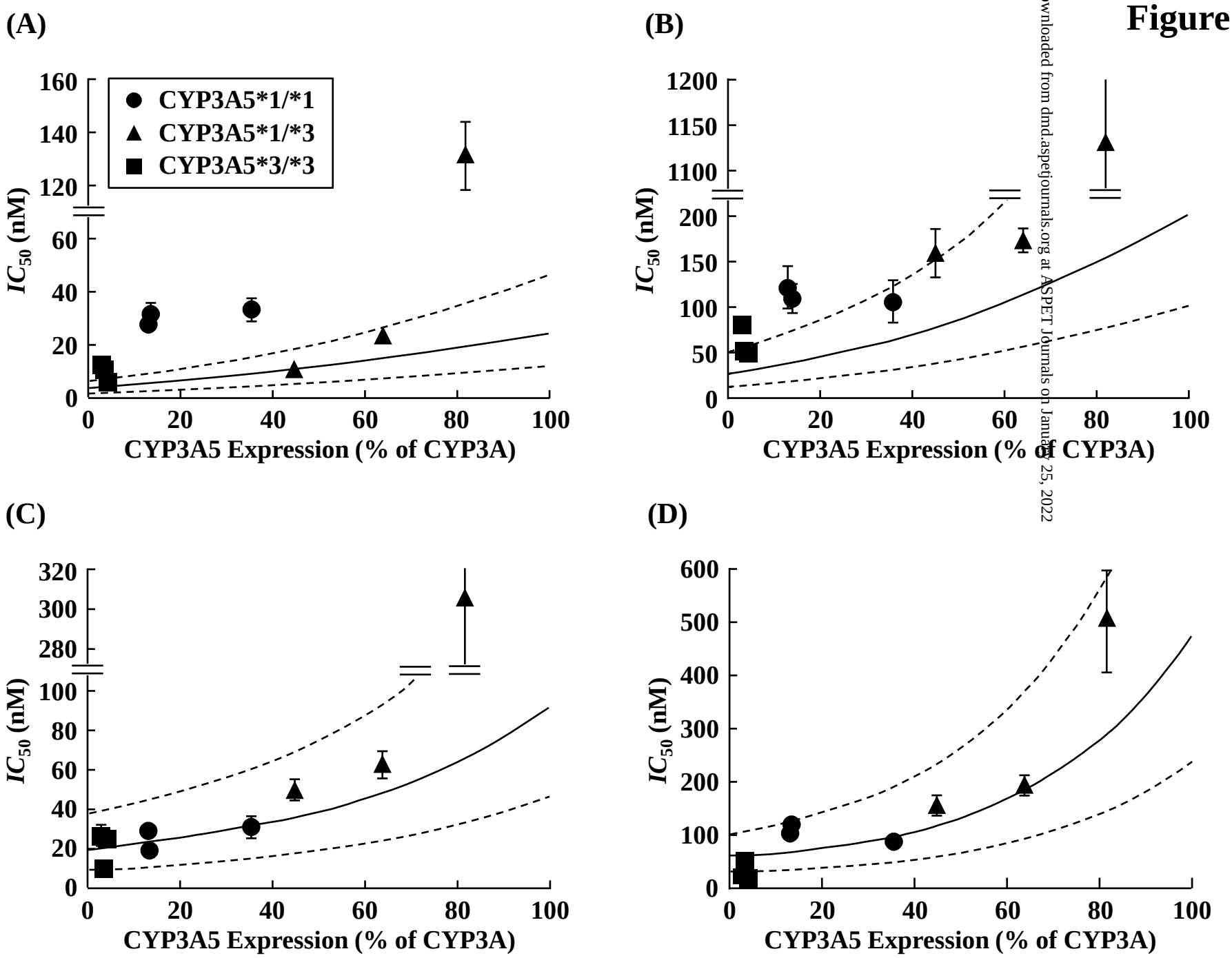

Figure 2

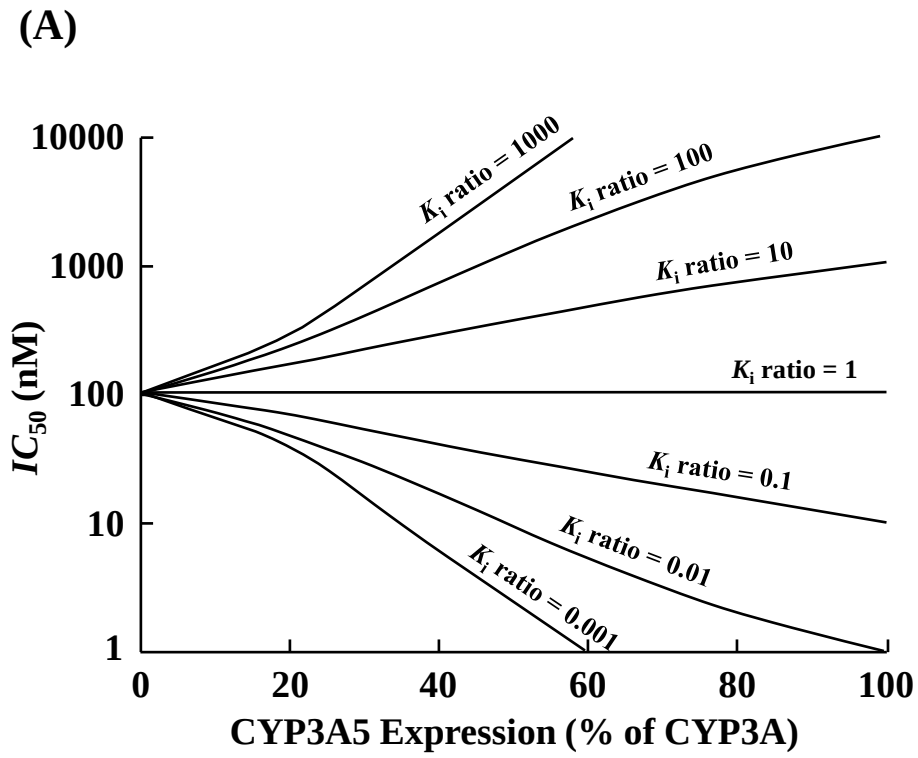

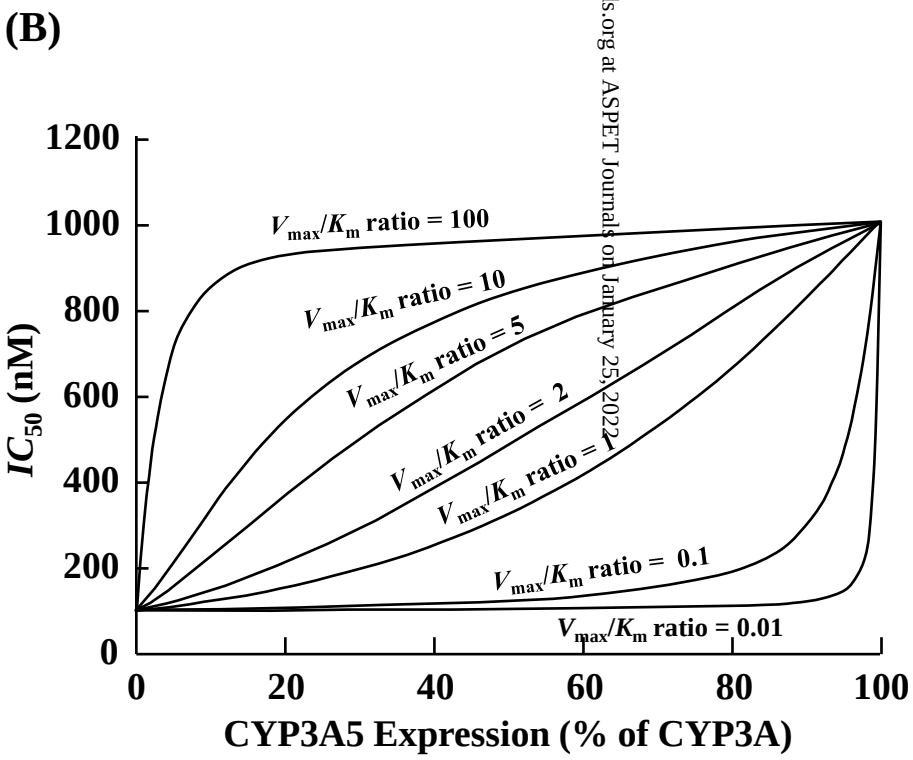

Supplementary Methods, Tables, and Figures

Effect of CYP3A5 Expression on the Inhibition of CYP3A-Catalyzed Drug Metabolism: Impact on CYP3A-Mediated Drug-Drug Interactions

Yoshiyuki Shirasaka, Shu-Ying Chang, Mary F. Grubb, Stephen R. Johnson, Chi-Chi Peng, Kenneth E. Thummel, Nina Isoherranen, and A. David Rodrigues

Inhibition of MDZ 1'-Hydroxylase and TST 6β-Hydroxylase Activity in HLM of *CYP3A5* Genotyped Livers. *Assessment of CYP3A inhibition*. The inhibitory effect of KTZ and ITZ on CYP3A-catalyzed metabolism of MDZ and TST was evaluated using HLMs. The IC_{50} value for KTZ and ITZ in HLM was measured using 1'-hydroxylation of midazolam (1'OH-MDZ) and 6β-hydroxylation of testosterone (6βOH-TST) as probe reactions for CYP3A-catalyzed metabolism. Incubations of each HLM with MDZ or TST were performed in solutions containing 100 mM potassium phosphate buffer (pH 7.4) with 1 mM EDTA in a shaking water bath maintained at 37°C. Conditions that conferred linear metabolite formation, with respect to time under different substrate and HLM protein concentrations, were determined (data not shown) and applied to all kinetic experiments described in this study.

For inhibition experiments with HLM using MDZ as a substrate, MDZ was used at 1 μM, and incubated for 5 min with 0.05 mg/mL HLM protein in a final volume of 100 μL. KTZ and ITZ were added to the 100 μL incubations at final concentrations of 3-3000 nM. All substrates and inhibitors were dissolved in acetonitrile; the final acetonitrile concentration was less than 1%. All reactions were initiated by adding NADPH (final concentration: 1 mM) after 10 min of preincubation and were terminated by adding an equal volume (100 μL) of ice-cold acetonitrile. All incubations were carried out in triplicate. The concentration of 1'OH-MDZ in all samples was quantified with a liquid chromatography-tandem mass spectrometry (LC/MS/MS) system consisting of MDS-Sciex API 3200® triple quadrupole mass spectrometer (AB Sciex, Foster City, CA) coupled with a LC-20AD® ultra fast liquid chromatography (UFLC) system (Shimadzu Co., Kyoto, Japan). The UFLC gradient elution was performed using a mobile phase composed of 0.1% formic acid (A) and acetonitrile (B) at a flow rate of 0.4 mL/min. The gradient profile was 10% B for 0-0.5 min, 10-90% B for 0.5-3.5 min, 90% B for 3.5-5.0 min, 90-10% B for 5.0-5.1 min, and 5.0% B for 5.1-7.0 min. The total run time was 7.0 min for each injection. The retention time of 1'OH-MDZ was 4.0 min. Hypersil GOLD (1.9 μm, 100 × 2.1 mm, Thermo, West Palm Beach, FL) was used as the analytical column. In the LC/MS/MS system, the Turbo Ion Spray interface was operated in the positive ion mode at 5500 V and 450˚C. The mass transition (Q1/Q3) of *m*/*z* 342.107/324.200 was used for 1'OH-MDZ. Analyst software version 1.4 was used for data analysis.

For inhibition experiments with HLM using TST as a substrate, TST was used at 10 μM, and incubated for 10 min with 0.05 mg/mL HLM protein in a final volume of 100 μL. KTZ and ITZ were added to the 100 μL incubations at final concentrations of 1-3000 nM. All substrates and inhibitors were dissolved in acetonitrile; the final acetonitrile concentration was less than 1%. All reactions were initiated by adding NADPH (final concentration: 1 mM) after 10 min of preincubation and were terminated by adding an equal volume (100μL) of ice-cold acetonitrile. All incubations were carried out in triplicate. The concentration of 6βOH-TST in all samples was quantified with a liquid chromatography-tandem mass spectrometry (LC/MS/MS) system consisting of MDS-Sciex API 3200® triple quadrupole mass spectrometer (AB Sciex, Foster City, CA) coupled with a LC-20AD® ultra fast

liquid chromatography (UFLC) system (Shimadzu Co., Kyoto, Japan). The UFLC gradient elution was performed using a mobile phase composed of 0.1% formic acid (A) and acetonitrile (B) at a flow rate of 0.3 mL/min. The gradient profile was 5.0% B for 0-2.0 min, 5.0-100% B for 2.0-4.0 min, 100% B for 4.0-5.5 min, 100-5.0% B for 5.5-5.6 min, and 5.0% B for 5.6-9.0 min. The total run time was 9.0 min for each injection. The retention time of 6βOH-TST was 4.5 min. ZORBAX (SB-C_{18} 5 µm, 2.1 x 50 mm, Agilent Technologies, Palo Alto, CA) was used as the analytical column. In the LC/MS/MS system, the Turbo Ion Spray interface was operated in the positive ion mode at 5500 V and 450˚C. The mass transition (Q1/Q3) of *m*/*z* 305.186/287.200 was used for 6βOH-TST. Analyst software version 1.4 was used for data analysis.

Determination of IC_{50}. The inhibitory effects of KTZ and ITZ on CYP3A-catalyzed metabolism of MDZ and TST were expressed as percent of control activity. Percent of control activity was determined as the ratio of the amount of 1'OH-MDZ and 6βOH-TST in the presence to that in the absence of KTZ or ITZ. The KTZ and ITZ concentrations giving half-maximum inhibition (IC_{50}) were obtained by means of nonlinear least-squares analysis using Graphpad prism (Peng et al 2012) or the MULTI program (Yamaoka et al., 1981).

Peng CC, Shi W, Lutz JD, Kunze KL, Liu JO, Nelson WL, and Isoherranen N (2012) Stereospecific metabolism of itraconazole by CYP3A4: dioxolane ring scission of azole antifungals. *Drug Metab Dispos* **40**:426-435.

Yamaoka K, Tanigawara Y, Nakagawa T, and Uno T (1981) A pharmacokinetic analysis program (multi) for microcomputer. *J Pharmacobiodyn* **4**: 879-885.

Reconstitution of Purified Wild-Type and Mutant CYP3A4 with P450 Reductase and Cytochrome b_5. Purified CYP3A4 (wild-type, mutant F213W, and L211F/D214E) was reconstituted with purified NADPH-P450 reductase, and cytochrome b_5 (molar ratio of 1:4:2), as described previously (Domanski et al, 2001), in the presence of 3-[(3-cholamidopropyl)dimethylammonio]-1-propanesulfonate (4%) and dioleoyl phosphatidylcholine (0.1 mg/mL) in 100 mM 3-(N-morpholino)propanesulfonic acid buffer (pH 7.6). TST 6β-hydroxylase activity (TST concentration of 25 and 100 µM) was determined after dilution of the reconstitution mixture in 50 mM 4-(2-hydroxyethyl)-1-piperazineethanesulfonic acid (pH 7.6) containing $MgCl_2$ (15 mM) and 0.1 mg/mL dioleoyl phosphatidylcholine. The final concentration of CYP3A4, P450 reductase and cytochrome b_5 was 0.5, 2, and 1 nM, respectively. The IC_{50} values for ITZ were obtained at two concentrations of TST (25 and 100 µM).

Domanski TL, He YA, Khan KK, Roussel F, Wang Q, and Halpert JR (2001) Phenylalanine and tryptophan scanning mutagenesis of CYP3A4 substrate recognition site residues and effect on substrate oxidation and cooperativity. *Biochemistry* **40**:10150-10160.

Determination of Ligand-Induced Binding Spectra. The binding mode and affinity of the ITZ and KTZ was determined by spectral titration with rCYP3A4 and rCYP3A5 Supersomes (Kunze et al., 2006). The ligand-induced binding spectra (difference spectra) were recorded with a Varian Cary 3E UV-Vis spectrophotometer. Matched cuvettes containing CYP3A4 or CYP3A5 Supersomes (200nM P450) in 100mM potassium phosphate buffer (pH 7.4) at 22°C were used. ITZ and KTZ (10 nM-6.5 µM) were added in 1 µL increments to the sample cuvette and the same volume of solvent (acetonitrile) was added to the reference cuvette. Ligand-induced difference spectra were recorded and, due to the tight binding of both azoles, the Ks values were obtained by fitting the "Morrison" equation (Eq. S1) to the spectral titration data. The enzyme-ligand (EL) complex concentration was determined by Lambert-

Beer law using the extinction coefficient determined from maximum absorbance detected when the P450 protein was saturated, as previously described (Kunze et al., 2006) (Eq. S1).

$$[\mathrm{EL}] = \frac{[\mathrm{E}] + [\mathrm{L}] + K_s - \sqrt{([\mathrm{E}] + [\mathrm{L}] + K_s)^2 - 4[\mathrm{E}]\ \mathrm{x}\ [\mathrm{L}]}}{2} \qquad \text{(S1)}$$

Ks is the affinity constant of the ligand, [L] is the concentration of ligand, [E] is the concentration of enzyme, and [EL] is the concentration of the enzyme-ligand complex.

Kunze KL, Nelson WL, Kharasch ED, Thummel KE, and Isoherranen N (2006) Stereochemical aspects of itraconazole metabolism in vitro and in vivo. *Drug Metab Dispos* **34**:583-590.

Table S1

Summary of Curve Fitting and IC_{50} Determination for KTZ with rCYP3A4 and rCYP3A5

Substrate	P450	[S]	Mean IC_{50}	±SD	R^2	Min	Max	Slope (y)
MDZ	CYP3A4	1.4	0.04	0.01	0.996	2.7	100	-1.5
		0.1	0.002	0.0002	0.999	0	100	-1.0
	CYP3A5	2.7	0.2	0.004	0.999	0	100	-0.9
		0.2	0.017	0.003	0.993	0	100	-0.9
TST	CYP3A4	78	0.009	0.001	0.990	0	100	-0.7
		4	0.016	0.0007	0.997	0	100	-1.3
	CYP3A5	67	0.04	0.006	0.991	0	100	-0.7
		3	0.08	0.007	0.986	0	100	-0.8
Terfenadine	CYP3A4	2.4	0.09	0.005	0.999	0	100	-1.0
		0.2	0.0082	0.001	0.996	0	100	-0.9
	CYP3A5	1.2	0.2	0.005	0.999	0	100	-0.9
		0.1	0.0065	0.002	0.968	0	100	-0.7
Vincristine	CYP3A4	85	0.15	0.03	0.970	0	100	-1.3
		4	0.11	0.01	0.991	0	100	-2.3
	CYP3A5	45	0.12	0.01	0.997	0	100	-0.6
		2	0.07	0.01	0.983	0	100	-2.1

IC_{50} values (± SD) were obtained at two [S] by means of nonlinear least-squares analysis (Eq. S2) using XLfit (IDBS, Guildford, UK).

$$y = \min + \frac{\max - \min}{1 + \left(\frac{x}{IC_{50}}\right)^{-y}} \quad \text{(S2)}$$

Where IC_{50} is the "*x*" value for the point in the curve that is midway between the "*max*" (maximum activity remaining; minimal % inhibition) and "*min*" (minimal activity remaining; maximal % inhibition). The exponent "*y*" is the slope of the curve at its midpoint. IC_{50} plots are shown (Figures S2 and S4).

Table S2

Summary of Curve Fitting and IC_{50} Determination for ITZ with rCYP3A4 and rCYP3A5

Substrate	P450	[S]	Mean IC_{50}	±SD	R^2	Min	Max	Slope (y)
MDZ	CYP3A4	1.4	0.24	0.05	0.999	5.3	100	-1.4
		0.1	0.005	0.001	0.984	0	100	-0.7
	CYP3A5	2.7	2.3	0.4	0.987	0	100	-0.7
		0.2	0.15	0.04	0.994	0	100	-0.9
TST	CYP3A4	78	0.04	0.007	0.985	0	100	-1.1
		4	0.045	0.003	0.995	0	100	-1.3
	CYP3A5	67	1.3	0.4	0.967	0	100	-0.8
		3	0.41	0.18	0.940	0	100	-0.4
Terfenadine	CYP3A4	2.4	0.9	0.2	0.999	16	100	-1.7
		0.2	0.023	0.004	0.995	0	100	-1.0
	CYP3A5	1.2	2.1	0.5	0.999	33	100	-2.0
		0.1	0.064	0.014	0.972	0	100	-0.8
Vincristine	CYP3A4	85	0.36	0.05	0.986	0	100	-0.9
		4	0.029	0.004	0.993	0	100	-1.7
	CYP3A5	45	0.68	0.23	0.926	0	100	-0.6
		2	0.05	0.005	0.992	0	100	-1.0

IC_{50} values (± SD) were obtained at two [S] by means of nonlinear least-squares analysis (Eq. S2) using XLfit (IDBS, Guildford, UK).

$$y = \min + \frac{\max - \min}{1 + \left(\frac{x}{IC_{50}}\right)^{-y}} \quad \text{(S2)}$$

Where IC_{50} is the "*x*" value for the point in the curve that is midway between the "*max*" (maximum activity remaining; minimal % inhibition) and "*min*" (minimal activity remaining; maximal % inhibition). The exponent "*y*" is the slope of the curve at its midpoint. IC_{50} plots are shown (Figures S1 and S3).

Table S3

ITZ as an Inhibitor of Fully Reconstituted Wild-Type and Mutant CYP3A4

CYP3A4 Preparation	Kinetic Profile[b]	IC_{50} (nM)[a] TST (25 μM)	IC_{50} (nM)[a] TST (100 μM)
Wild-Type	Sigmoidal	81 ± 16	140 ± 62
F213W	NR	92 ± 30[c]	79 ± 14[d]
L211F/D214E	Hyperbolic	65 ± 7.0[c]	80 ± 13[*]

[a]IC_{50} was determined at two concentrations of TST and is presented as the mean ± S.D. (n = 3 determinations).
[b]TST profile reported previously for wild-type and L211F/D214E forms of CYP3A4 (Harlow and Halpert, 1998).
NR: Not reported.
[c]Not statistically significant versus wild-type (P = 0.16, L211F/D214E; P = 0.26, F213W).
[d]Not statistically significant versus wild-type (P = 0.05).
* P <0.05 (P = 0.04), significantly different from wild-type CYP3A4.

Harlow GR and Halpert JR (1998) Analysis of human cytochrome P450 3A4 cooperativity: construction and characterization of a site-directed mutant that displays hyperbolic steroid hydroxylation kinetics. *Proc Natl Acad Sci U S A* **95**: 6636-6641.

Supplement Figure S1

Representative IC_{50} plots describing the inhibition of rCYP3A4- and rCYP3A5-catalyzed metabolism of MDZ, TST, terfenadine and vincristine by ITZ ([S]/K_m ratio ~1.0)

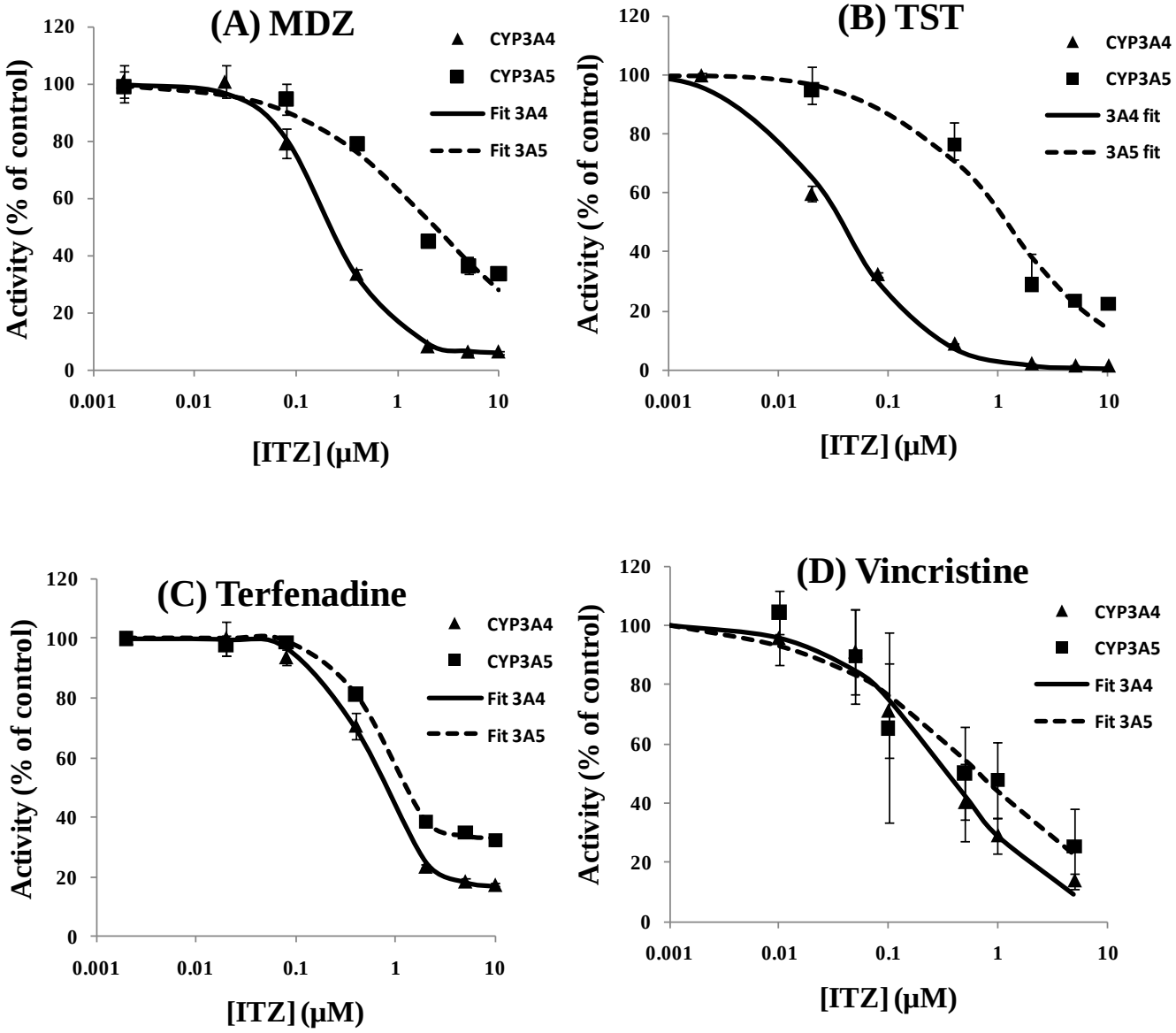

Supplement Figure S2

Representative IC_{50} plots describing the inhibition of rCYP3A4- and rCYP3A5-catalyzed metabolism of MDZ, TST, terfenadine and vincristine by KTZ ([S]/K_m ratio ~1.0)

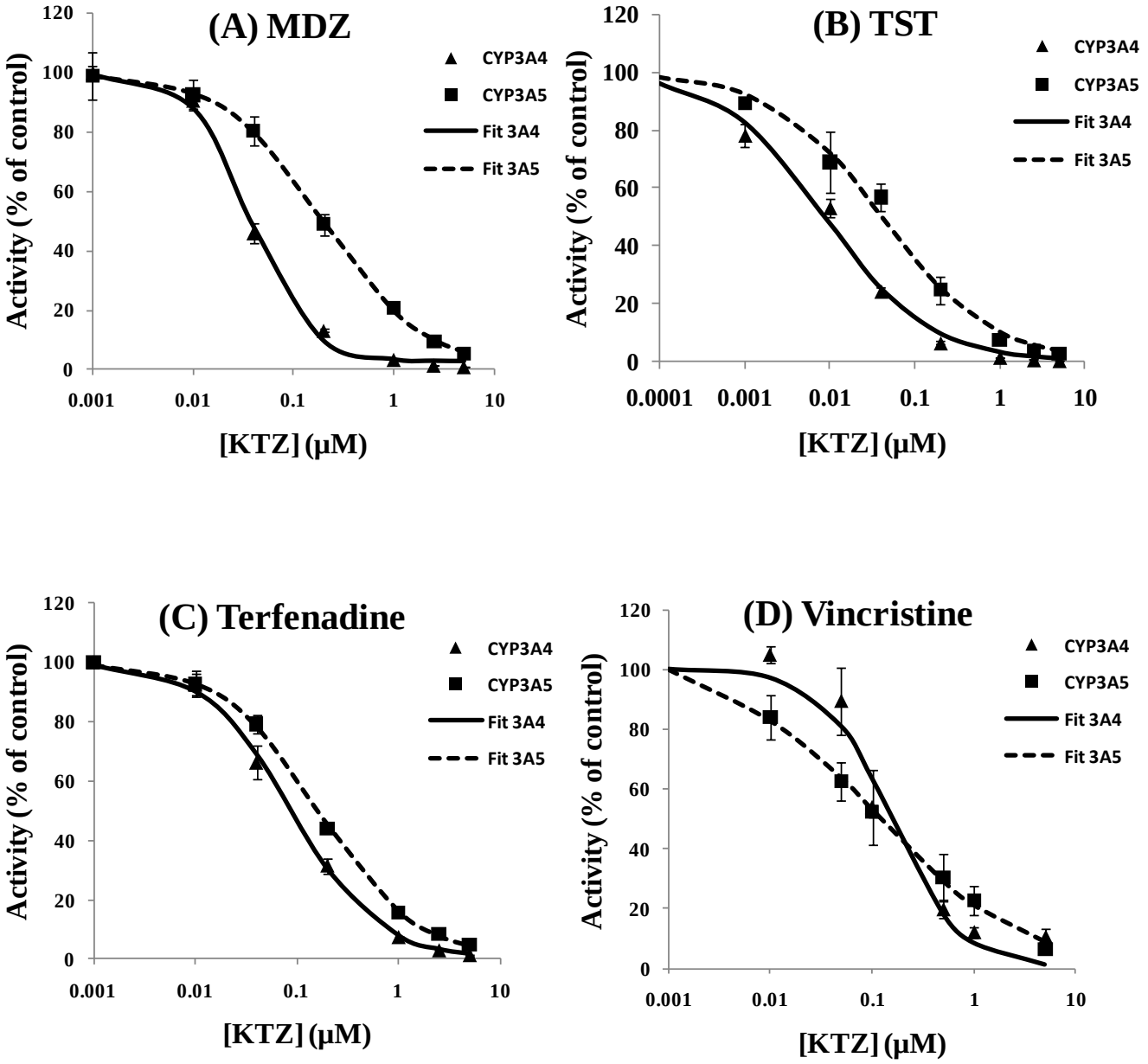

Supplement Figure S3

Representative IC_{50} plots describing the inhibition of rCYP3A4- and rCYP3A5-catalyzed metabolism of MDZ, TST, terfenadine and vincristine by ITZ ([S]/K_m ratio ~0.05)

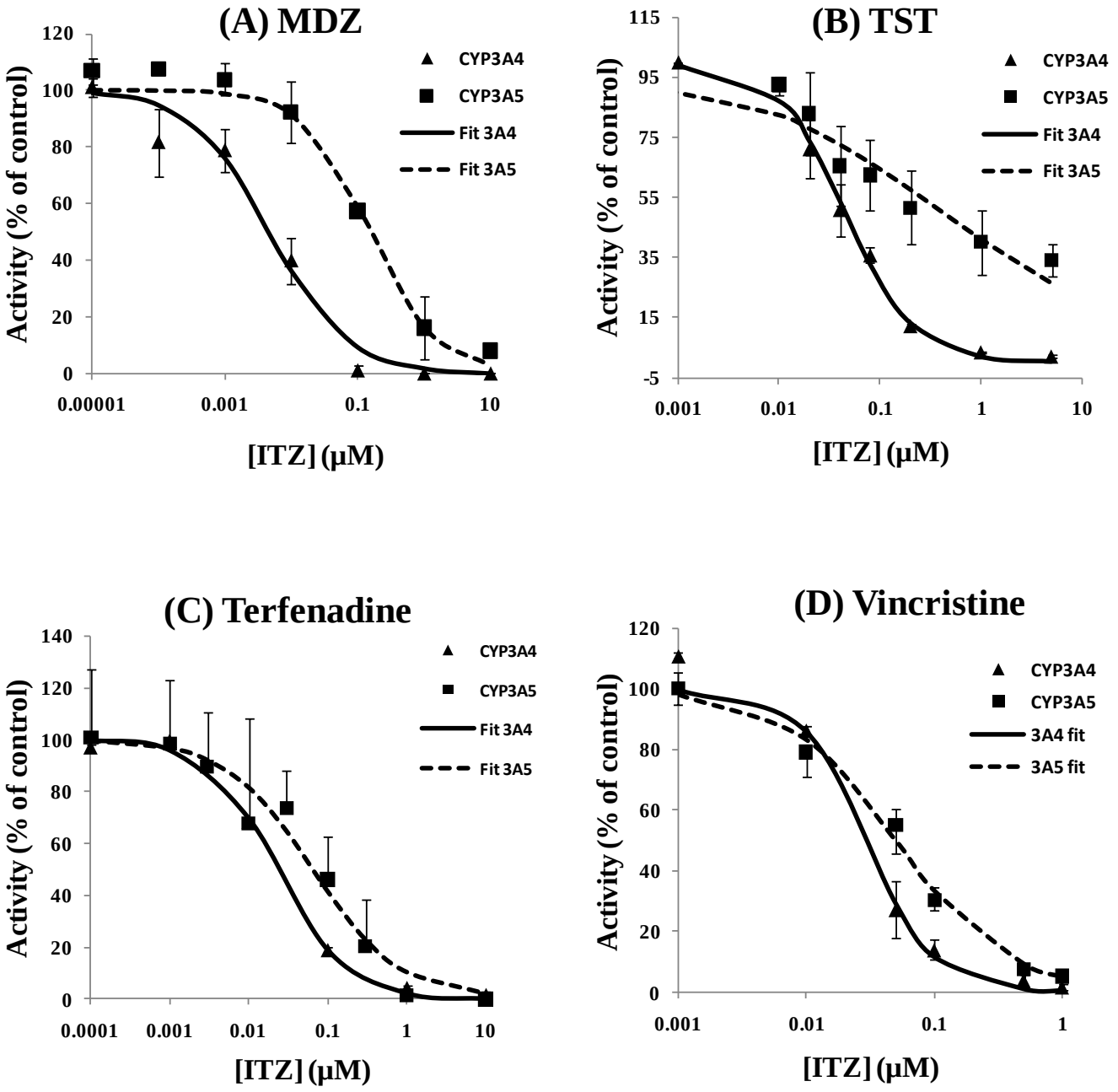

Supplement Figure S4

Representative IC_{50} plots describing the inhibition of rCYP3A4- and rCYP3A5-catalyzed metabolism of MDZ, TST, terfenadine and vincristine by KTZ ([S]/K_m ratio ~0.05)

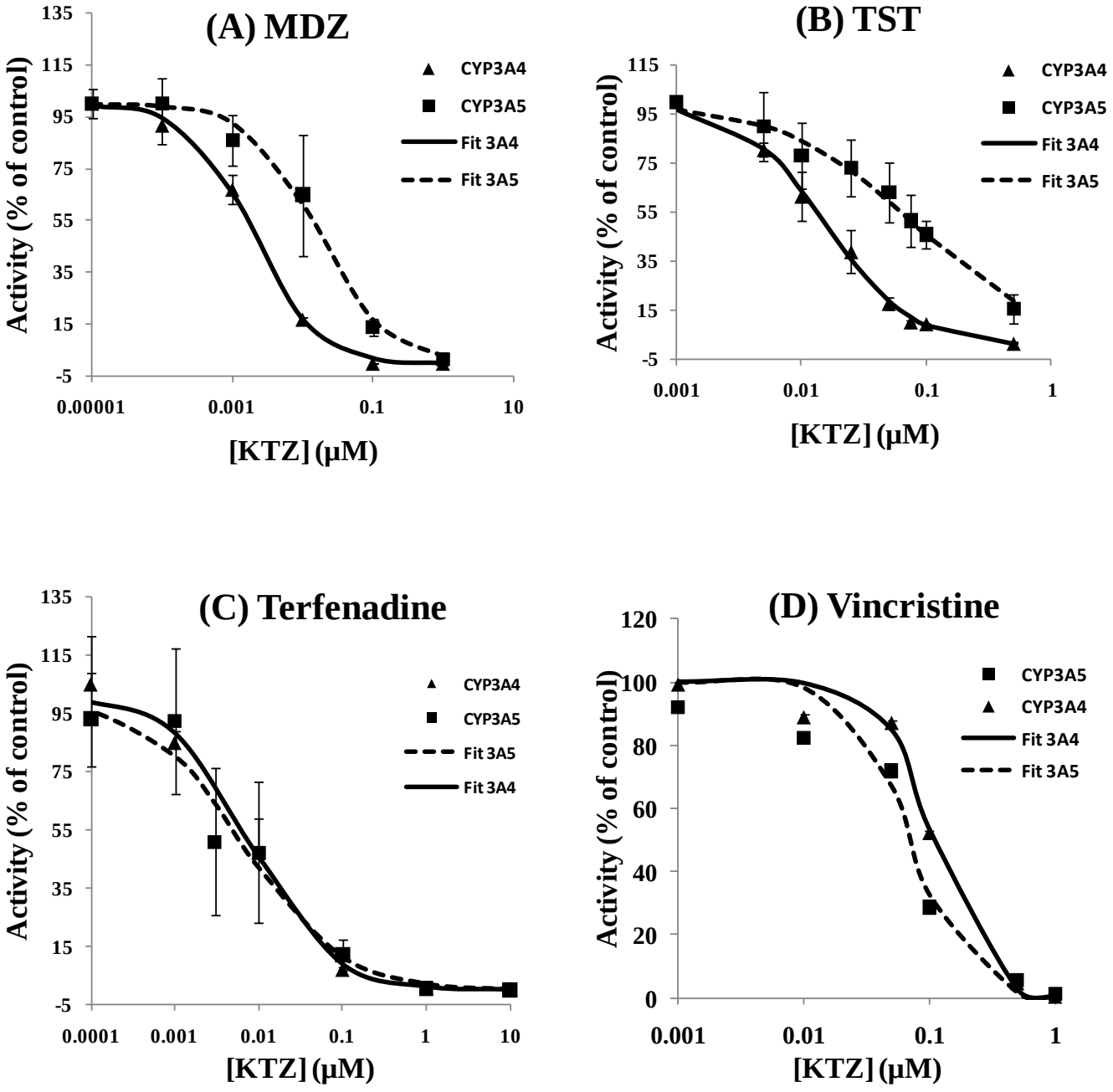

Supplement Figure S5

Representative Type II ligand spectral titration plot for ITZ with rCYP3A4 (A) and rCYP3A5 (B) and KTZ with rCYP3A4 (C) and rCYP3A5 (D)

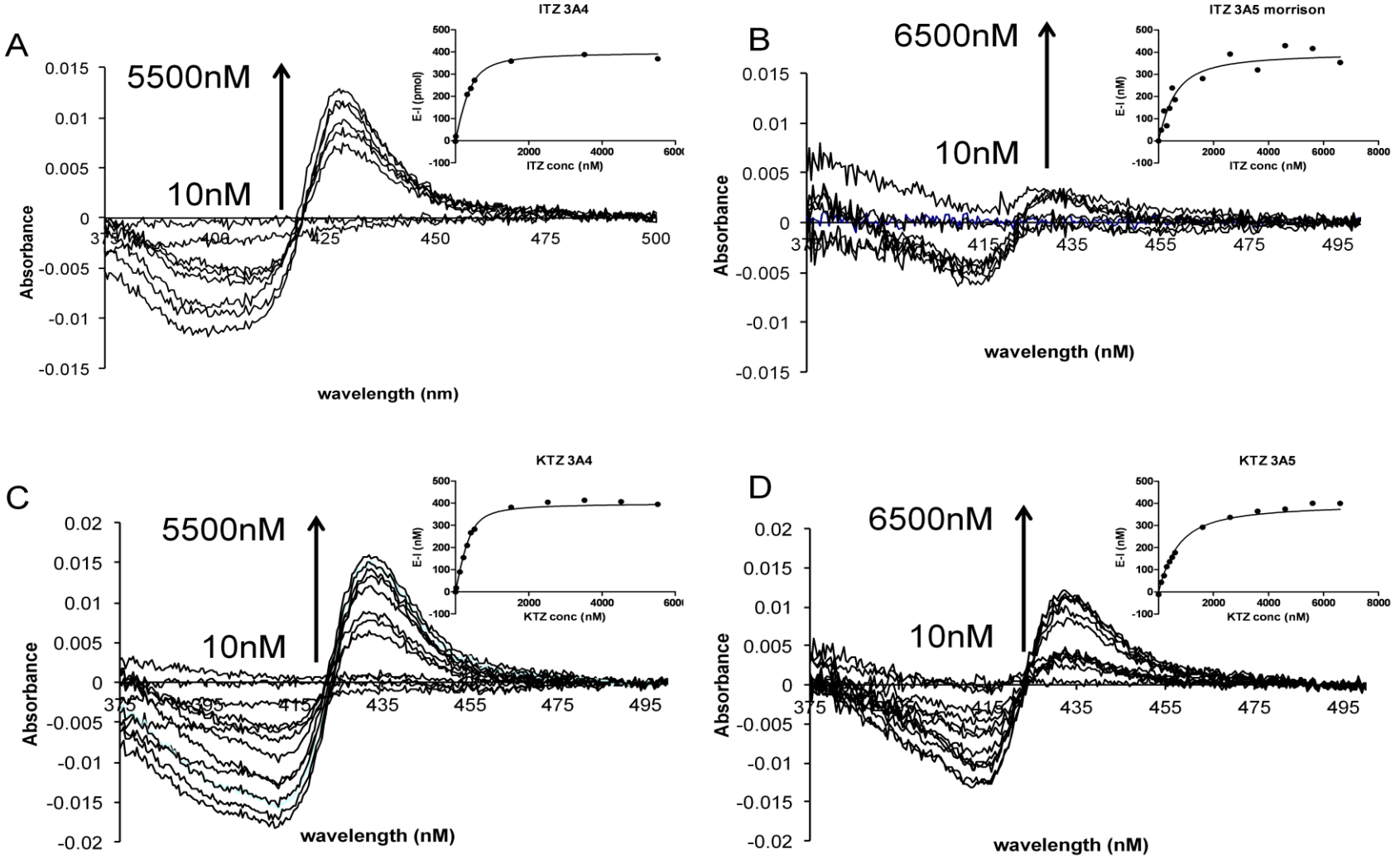

Supplement Figure S6

Representative IC_{50} plots describing the inhibition wild-type and mutant CYP3A4-catalyzed TST (25 and 100 µM) metabolism by ITZ

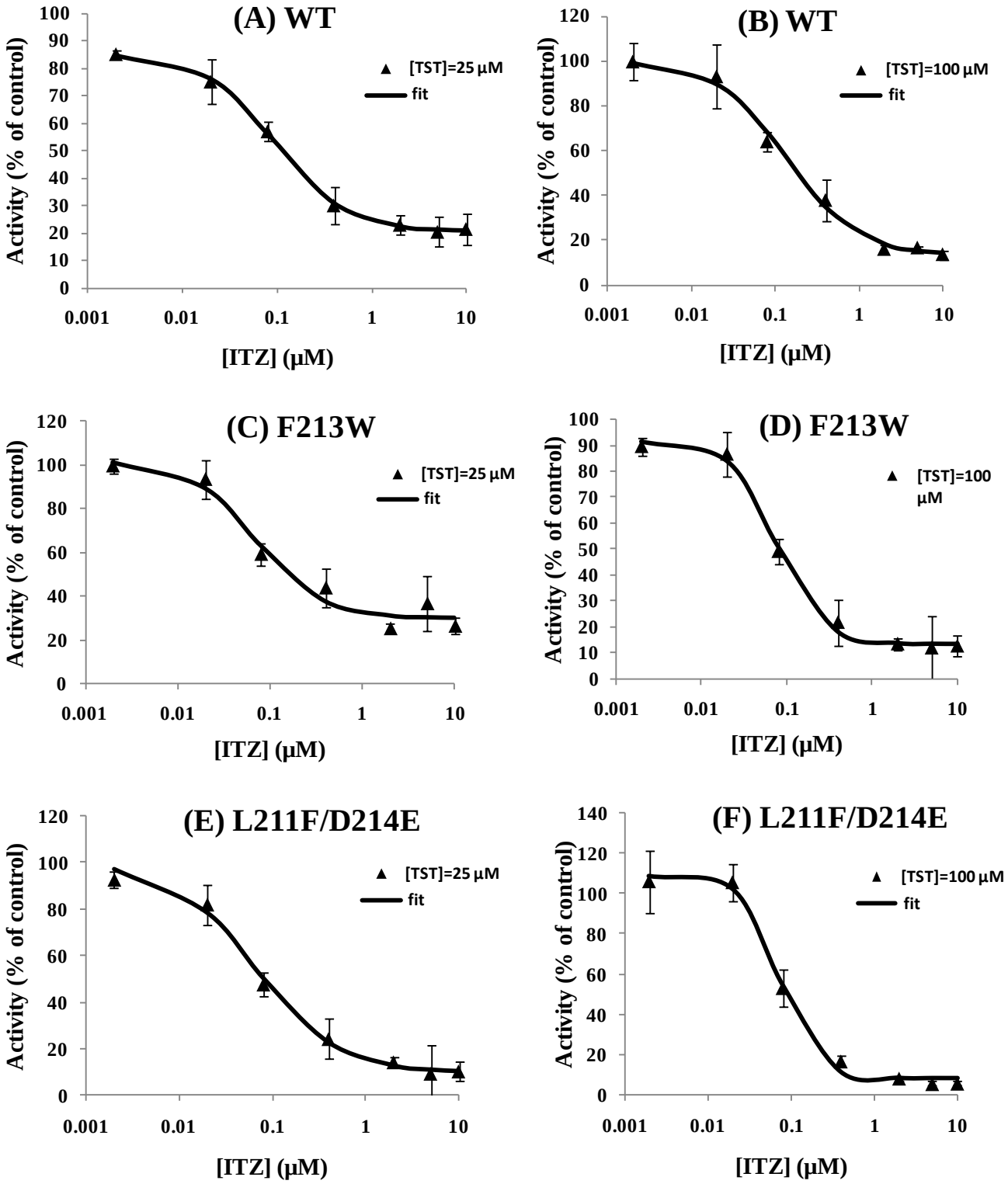

Supplement Figure S7

Representative IC_{50} plots describing the inhibitory effect of KTZ and ITZ on CYP3A-catalyzed metabolism of MDZ in HLM

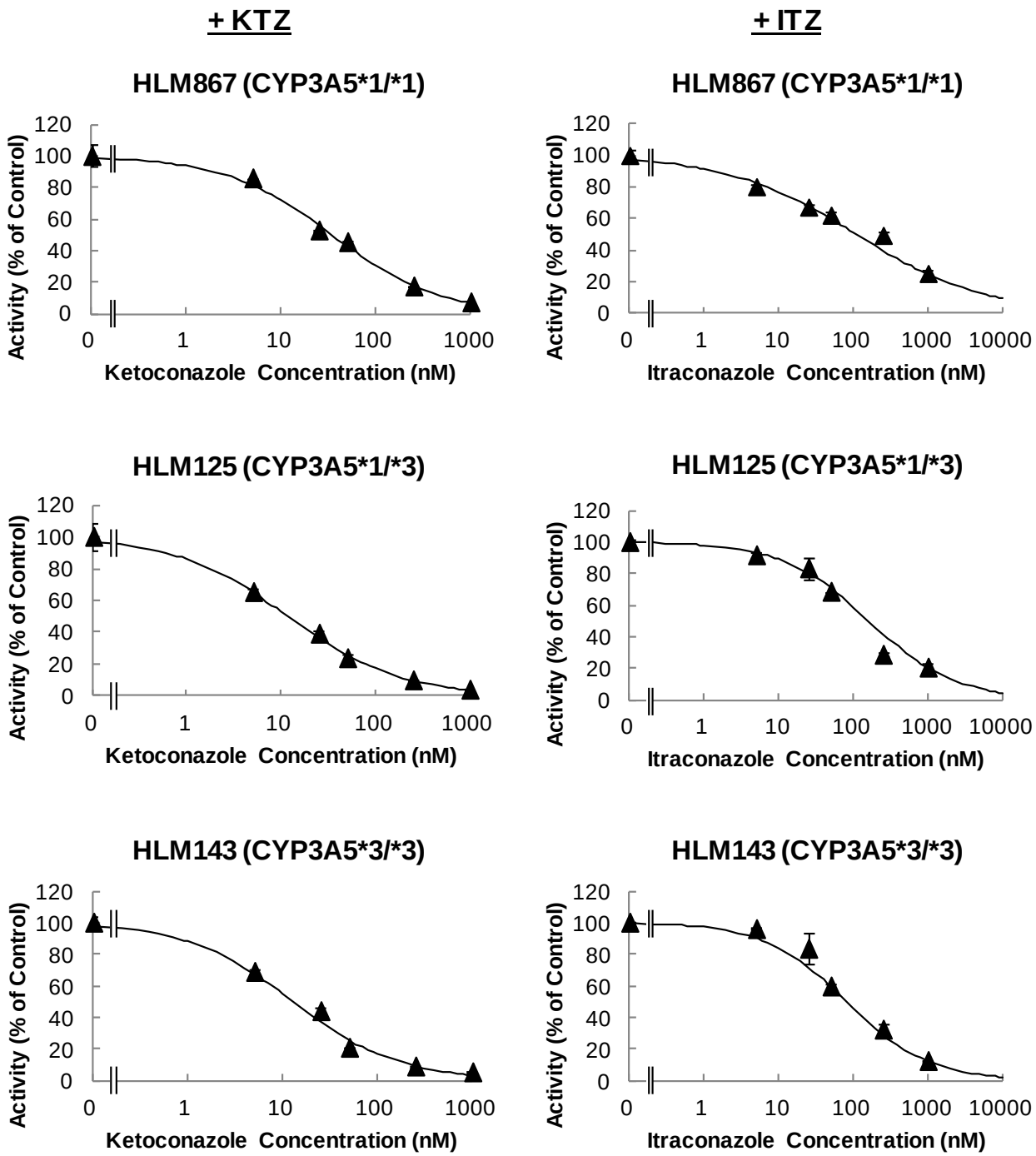

Supplement Figure S8

Representative IC_{50} plots describing the inhibitory effect of KTZ and ITZ on CYP3A-catalyzed metabolism of TST in HLM